The Long-Term Dynamical Evolution of Planetary Systems

Melvyn B. Davies
Lund University

Fred C. Adams
University of Michigan

Philip Armitage
University of Colorado, Boulder

John Chambers
Carnegie Institution of Washington

Eric Ford
The Pennsylvania State University, University of Florida

Alessandro Morbidelli
University of Nice

Sean N. Raymond
University of Bordeaux

Dimitri Veras
University of Cambridge

This chapter concerns the long-term dynamical evolution of planetary systems from both theoretical and observational perspectives. We begin by discussing the planet-planet interactions that take place within our own Solar System. We then describe such interactions in more tightly-packed planetary systems. As planet-planet interactions build up, some systems become dynamically unstable, leading to strong encounters and ultimately either ejections or collisions of planets. After discussing the basic physical processes involved, we consider how these interactions apply to extrasolar planetary systems and explore the constraints provided by observed systems. The presence of a residual planetesimal disc can lead to planetary migration and hence cause instabilities induced by resonance crossing; however, such discs can also stabilise planetary systems. The crowded birth environment of a planetary system can have a significant impact: close encounters and binary companions can act to destabilise systems, or sculpt their properties. In the case of binaries, the Kozai mechanism can place planets on extremely eccentric orbits which may later circularise to produce hot Jupiters.

1. INTRODUCTION

Currently observed planetary systems have typically evolved between the time when the last gas in the protoplanetary disc was dispersed, and today. The clearest evidence for this assertion comes from the distribution of Kuiper belt objects in the outer solar system, and from the eccentricities of massive extrasolar planets, but many other observed properties of planetary systems may also plausibly be the consequence of dynamical evolution. This chapter summarizes the different types of gravitational interactions that lead to long-term evolution of planetary systems, and reviews the application of theoretical models to observations of the solar system and extrasolar planetary systems.

Planetary systems evolve due to the exchange of angular momentum and / or energy among multiple planets, between planets and disks of numerous small bodies ("planetesimals"), between planets and other stars, and via tides with the stellar host. A diverse array of dynamical evolution ensues. In the simplest cases, such as a well-separated two planet system, the mutual perturbations lead only to periodic oscillations in the planets' eccentricity and inclination. Of greater interest are more complex multiple planet systems where the dynamics is chaotic. In different circumstances the chaos can lead to unpredictable (but bounded) excursions in planetary orbits, to large increases in eccentricity as the system explores the full region of phase space allowed by conservation laws, or to close approaches between planets resulting in collisions or ejections. Qualitative changes to the architecture of planetary systems can likewise be caused by dynamical interactions in binary systems, by stellar encounters in clusters, or by changes to planetary orbits due to interactions with planetesimal discs.

Theoretically, there has been substantial progress since the last *Protostars and Planets* meeting in understanding the dynamics that can reshape planetary systems. Observational progress has been yet more dramatic. Radial velocity surveys and the Kepler mission have provided extensive catalogues of single and multiple planet systems, that can be used to constrain the prior dynamical evolution of planetary systems (see the chapter by *Fischer et al.* for more details). Routine measurements of the Rossiter-McLaughlin effect for transiting extrasolar planets have shown that a significant fraction of hot Jupiters have orbits that are misaligned with respect to the stellar rotation axis, and have prompted new models for how hot Jupiters form. Despite this wealth of data, the relative importance of different dynamical processes in producing what we see remains unclear, and we will discuss in this review what new data is needed to break degeneracies in the predictions of theoretical models. Also uncertain is which observed properties of planetary systems reflect dynamical evolution taking place subsequent to the dispersal of the gas disk (the subject of this chapter), and which involve the coupled dynamics and *hydrodynamics* of planets, planetesimals and gas within the protoplanetary disc. The chapter by *Baruteau et al*. (2013) reviews this earlier phase of evolution.

We begin this chapter by considering the long term stability of the solar system. The solar system is chaotic, but our four giant planets are fundamentally stable, and there is only a small probability that the terrestrial planets will experience instability during the remaining main-sequence lifetime of the Sun. We then compare the current solar system to more tightly-packed planetary systems, which are hypothesized progenitors to both the solar system and extrasolar planetary systems. We discuss the conditions, time scales and outcomes of the dynamical instabilities that can be present in such systems, and compare theoretical models to the observed population of extrasolar planets. We then review how interactions between planets and residual planetesimal disks can lead to planetary migration, which depending on the circumstances can either stabilize or destabilize a planetary system. Finally we discuss the outcome of dynamical interactions between planetary systems and other stars, whether bound in binaries or interlopers that perturb planets around stars in stellar clusters. Dynamical evolution driven by inclined stellar-mass (and possibly substellar or planetary-mass) companions provides a route to the formation of hot Jupiters whose orbits are misaligned to the stellar equator, and we review the status of models for this process (often called the Kozai mechanism). We close with a summary of the key points of this chapter.

2. THE SOLAR SYSTEM TODAY

A quick glance at our system, with the planets moving on quasi-circular and almost coplanar orbits, well separated from each other, suggests the idea of a perfect clockwork system, where the orbital frequencies tick the time with unsurpassable precision. But is it really so? In reality, due to their mutual perturbations, the orbits of the planets must vary over time.

To a first approximation, these variations can be described by a secular theory developed by Lagrange and Laplace (see *Murray and Dermott* 1999) in which the orbital elements that describe a fixed Keplerian orbit change slowly over time. The variations can be found using Hamilton's equations, expanding the Hamiltonian in a power series in terms of the eccentricity e and inclination i of each planet, and neglecting high-frequency terms that depend on the mean longitudes. Only the lowest order terms are retained since e and i are small for the planetary orbits. The variations for a system of planets j (ranging from 1 to N) can then be expressed as

$$\begin{aligned} e_j \sin\varpi_j &= \sum_{k=1}^{N} e_{kj} \sin(g_k t + \beta_k) \\ e_j \cos\varpi_j &= \sum_{k=1}^{N} e_{kj} \cos(g_k t + \beta_k) \end{aligned} \qquad (1)$$

with similar expressions for i. Here ϖ is the longitude of perihelion, and the quantities e_{kj}, g_k, and β_k are determined by the planet's masses and initial orbits.

In the Lagrange-Laplace theory, the orbits' semi-major axes a remain constant, while e and i undergo oscillations with periods of hundreds of thousands of years. The orbits change, but the variations are bounded, and there are no long-term trends. Even at peak values, the eccentricities are small enough that the orbits do not come close to intersecting. Therefore, the Lagrange-Laplace theory concludes that the solar system is stable.

The reality, however, is not so simple. The Lagrange-Laplace theory has several drawbacks that limit its usefulness in real planetary systems. It is restricted to small values of e and i; theories based on higher order expansions exist, but they describe a much more complex time-dependence of eccentricities and inclinations, whose Fourier expansions involve harmonics with argument νt where $\nu = \sum_{k=1}^{N} n_k g_k + m_k s_k$ and n_k, m_k are integers, and g and s are secular frequencies associated with e and i respectively. The coefficients of these harmonics are roughly inversely proportional to ν, so that the Fourier Series representation breaks down when $\nu \sim 0$, a situation called *secular resonance*.

Moreover, the Lagrange-Laplace theory ignores the effects of mean-motion resonances or near resonances between the orbital periods of the planets. The existence of mean-motion resonances can fundamentally change the dynamics of a planetary system and alter its stability in ways not predicted by Lagrange-Laplace theory. In particular, the terms dependent on the orbital frequencies, ignored in the Lagrange-Laplace theory, become important when the ratio of two orbital periods is close to the ratio of two integers. This situation arises whenever the critical argument ϕ varies slowly over time, where

$$\phi = k_1\lambda_i + k_2\lambda_j + k_3\varpi_i + k_4\varpi_j + k_5\Omega_i + k_6\Omega_j \quad (2)$$

for planets i and j, where λ is the mean longitude, Ω is the longitude of the ascending node, and k_{1-6} are integers. The k_{3-6} terms are included because the orbits will precess in general, so a precise resonance is slightly displaced from the case where k_1/k_2 is a ratio of integers.

To leading order, the evolution at a resonance can be described quite well using the equation of motion for a pendulum (*Murray and Dermott* 1999):

$$\ddot{\phi} = -\omega^2 \sin\phi \quad (3)$$

At the centre of the resonance, ϕ and $\dot{\phi}$ are zero and remain fixed. When ϕ is slightly non-zero initially, ϕ librates about the equilibrium point with a frequency ω that depends on the amplitude of the librations. The semi-major axes and eccentricities of the bodies involved in the resonance undergo oscillations with the same frequency. There is a maximum libration amplitude for which ϕ approaches $\pm\pi$. At larger separations from the equilibrium point, ϕ circulates instead and the system is no longer bound in resonance.

Whereas a single resonance exhibits a well-behaved, pendulum-like motion as described above, when multiple resonances overlap the behavior near the boundary of each resonance becomes erratic, which leads to chaotic evolution. Because the frequencies of the angles $\varpi_{i,j}$ and $\Omega_{i,j}$ are small relative to the orbital frequencies (i.e. the frequencies of $\lambda_{i,j}$), in general resonances with the same k_1, k_2 but different values of $k_{3,\ldots,6}$ overlap with each other. Thus, quite generically, a region of chaotic motion can be found associated with each mean-motion resonance.

There are no mean-motion resonances between pairs of Solar System planets. Jupiter and Saturn, however, are close to the 2:5 resonance, and Uranus and Neptune are close to the 1:2 resonance. In both cases, the resonant angle ϕ is in circulation and does not exhibit chaotic motion. In general, systems can support N-body resonances, which involve integer combinations of the orbital frequencies of N planets, with $N > 2$. The forest of possible resonances becomes rapidly dense, and increases with the number N of planets involved. As a result, analytic models become inappropriate to describe precisely the dynamical evolution of a system with many planets.

Fortunately, modern computers allow the long-term evolution of the Solar System to be studied numerically using N-body integrations. These calculations can include all relevant gravitational interactions and avoid the approximations inherent in analytic theories. One drawback is that N-body integrations can never prove the stability of a system, only its stability for the finite length of an integration.

N-body integrations can be used to distinguish between regular and chaotic regions, and quantify the strength of chaos, by calculating the system's Lyapunov exponent Γ, given by

$$\Gamma = \lim_{t\to\infty} \frac{\ln[d(t)/d(0)]}{t} \quad (4)$$

where d is the separation between two initially neighboring orbits. Regular orbits diverge from one another at a rate that is a power of time. Chaotic orbits diverge exponentially over long timespans, although they can be "sticky", mimicking regular motion for extended time intervals. If the Solar System is chaotic, even a tiny uncertainty in the current orbits of the planets will make it impossible to predict their future evolution indefinitely.

One of the first indications that the Solar System is chaotic came from an 845 Myr integration of the orbits of the outer planets plus Pluto (*Sussman and Wisdom* 1988). Pluto was still considered a planet at the time due to its grossly overestimated mass. This work showed that Pluto's orbit is chaotic with a Lyapunov timescale ($T_L = 1/\Gamma$) of 20 My. Using a 200 Myr integration of the secular equations of motion, *Laskar* (1989) showed that the 8 major planets are chaotic with a Lyapunov time of 5 My. This result was later confirmed using full N-body integrations (*Sussman and Wisdom* 1992). The source of the chaos is due to the existence of two secular resonances, with frequencies $\nu_1 = 2(g_4 - g_3) - (s_4 - s_3)$ and $\nu_2 = (g_1 - g_5) - (s_1 - s_2)$, i.e. frequencies not appearing in the Lagrange-Laplace theory (*Laskar* 1990).

The four giant planets by themselves may be chaotic (*Sussman and Wisdom* 1992), due to a three-body resonance involving Jupiter, Saturn and Uranus (*Murray and Dermott* 1999). Assuming that the evolution can be described as a random diffusion through the chaotic phase space within this resonance, *Murray and Dermott* (1999) estimated that it will take $\sim 10^{18}$ y for Uranus's orbit to cross those of its neighbors. However, careful examination suggests that chaotic and regular solutions both exist within the current range of uncertainty for the orbits of the outer planets (*Guzzo* 2005; *Hayes* 2008), so the lifetime of this subsystem could be longer, and even infinite.

Numerical integrations can also be used to assess the long-term stability of the planetary system, with the caveat that the precise evolution can never be known, so that simulations provide only a statistical measure of the likely behavior. Numerical simulations confirm the expectation that the orbits of the giant planets will not change significantly over the lifetime of the Sun (*Batygin and Laughlin* 2008). Nonetheless, there remains a remote possibility that the orbits of the inner planets will become crossing on a timescale of a few Gyr (*Laskar* 1994, 2008; *Batygin and Laughlin* 2008; *Laskar and Gastineau* 2009).

In principle, if the terrestrial planets were alone in the solar system, they would be stable for all time. (In practice, of course, the Solar System architecture will change on a time scale of only ~ 7 Gyr due to solar evolution and mass loss.) In fact, even if the orbits of the inner planets are free to diffuse through phase space, their evolution would still be constrained by their total energy and angular momentum.

A useful ingredient in orbital evolution is the angular momentum deficit (AMD), given by

$$\mathrm{AMD} \equiv \sum_k \Lambda_k \left(1 - \cos i_k \sqrt{1 - e_k^2}\right) \qquad (5)$$

where $\Lambda_k = M_k M_* / (M_k + M_*) \sqrt{G(M_* + M_k) a_k}$ is the angular momentum of planet k with mass M_k, semi-major axis a_k, eccentricity e_k and inclination i_k to the invariable plane, and M_* is the mass of the host star.

In absence of mean-motion resonances, to a good approximation, a remains constant for each planet, so AMD is also constant (e.g. *Laskar* 1997, though this result dates to Laplace), Excursions in e and i are constrained by conservation of AMD, and the maximum values attainable by any one planet occur when all the others have $e = i = 0$. Mercury's low mass means it can acquire a more eccentric and inclined orbit than the other planets. However, even when Mercury absorbs all available AMD, its orbit does not cross Venus. However, when the giant planets are taken into account, the exchange of a small amount of angular momentum between the outer planets and the inner planets can give the latter enough AMD to develop mutual crossing orbits. As a result, long-term stability is not guaranteed.

The possible instability of the terrestrial planets on a timescale of a few Gyr shows that the solar system has not yet finished evolving dynamically. Its overall structure can still change in the future, even if marginally within the remaining main-sequence lifetime of the Sun.

This potential change in the orbital structure of the planets would not be the first one in the history of the solar system. In fact, several aspects of the current orbital architecture of the solar system suggest that the planetary orbits changed quite drastically after the epoch of planet formation and the disappearence of the proto-planetary disk of gas. For instance, as described above, the giant planets are not in mean motion resonance with each other. However, their early interaction with the disk of gas in which they formed could have driven them into mutual mean-motion resonances such as the 1:2, 2:3 or 3:4, where the orbital separations are much narrower than the current ones (*Lee and Peale* 2002; *Kley et al.* 2005; *Morbidelli et al.* 2007). We do indeed observe many resonant configurations among extra-solar planetary systems, and in numerical simulations of planetary migration. Also, the current eccentricities and inclinations of the giant planets of the solar system, even if smaller than those of many extra-solar planets, are nevertheless non-zero. In a disk of gas, without any mean-motion resonant interaction, the damping effects would have annihilated the eccentricities and inclinations of the giant planets in a few hundred orbits (*Kley and Dirksen* 2006; *Cresswell et al.* 2007). So, some mechanism must have extracted the giant planets from any original mean-motion resonances and placed them onto their current, partially eccentric and inclined orbits, after gas removal.

The populations of small bodies of the solar system also attest to significant changes in the aftermath of gas removal, and possibly several 100 Myr later. The existence and properties of these populations thus provide important constraints on our dynamical history (e.g., see Section 6). There are three main reservoirs of small bodies: the asteroid belt between Mars and Jupiter, the Kuiper belt immediately beyond Neptune and the Oort cloud at the outskirts of the solar system. At the present epoch, both the asteroid belt and the Kuiper belt contain only a small fraction of the mass (0.1% or less) that is thought to exist in these regions when the large objects that we observe today formed (*Kenyon and Bromley* 2004). As a result, the vast majority of the primordial objects (by number) have been dynamically removed. Some of these bodies were incorporated into the forming planets, some were scattered to other locations within the solar system, and some where ejected. The remaining objects (those that make up the current populations of the asteroid and Kuiper belts) are dynamically excited, in the sense that their eccentricities and inclinations cover the entire range of values allowed by long-term stability constraints; for instance, the inclinations can be as large as 40 degrees, much larger than the nearly-co-planar orbits of the planets themselves. This evidence suggests that some dynamical mechanism removed more than 99.9% of the objects and left the survivors on excited orbits, much different from their original circular and co-planar ones. Another constaint is provided by the absence of a correlation between the size of the objects and their orbital excitation. Presumably, the mechanism that altered the orbits of these small bodies acted *after* the removal of the nebular gas; otherwise, gas drag, which is notoriously a size-dependent process, would have imprinted such a correlation. Similarly, the Oort cloud (the source of long period comets) contains hundreds of billions of kilometer-size objects, and most trace through orbits with high eccentricities and inclinations (*Wiegert and Tremaine* 1999; *Kaib and Quinn* 2009). Since the Oort cloud extends far beyond the expected size of circumstellar disks, the population is thought to have been scattered to such large distances. In the presence of gas, however, these small objects could not have been scattered out by the giant planets, because gas-drag would have circularized their orbits just beyond the giant planets (*Brasser et al.* 2007). Thus, presumably the formation of the Oort cloud post-dates gas removal; this timing is consistent with considerations of the Solar birth environment (Section 6).

Finally, there is evidence for a surge in the impact rates and/or impact velocities on the bodies of the inner solar system, including the terrestrial planets, the Moon, and the asteroid Vesta (*Tera et al.* 1974; *Ryder* 2002; *Kring and Cohen* 2002; *Marchi et al.* 2012a,b, 2013). This surge seems to have occurred during a time interval ranging from 4.1 to 3.8 Gyr ago, i.e., starting about 400 Myr after planet formation. This event is often referred to as the "terminal Lunar Cataclysm" or the "Late Heavy Bombardment". If such a cataclysm really happened (its existence is still debated today; see for instance *Hartmann et al.* 2000), it suggests that the changes in the structure of the solar system described above did not happen immediately after the removal of gas from the early solar nebula, but only after a significant delay of several 100 Myr.

All of this discussion provides hints that the mechanisms of orbital instability discussed in the next sections of this chapter in the framework of extra-solar planets evolution were probably not foreign to the solar system. Specifically, a scenario of possible evolution of the solar system that explains all these aspects will be presented in Section 5.

3. INSTABILITIES IN TIGHTLY-PACKED SYSTEMS

We will see in this section that the timescale for planetary system to become unstable is a very sensitive function of planetary separations. Thus the separations of planets within a system is an important quantity. Unfortunately, the typical separation of planets in newly-formed planetary systems is unknown observationally and theoretical predictions are also unclear. For terrestrial planets whose final assembly occurs after gas disk dispersal, the results of *Kokubo and Ida* (1998) suggest that separations of $\simeq 10$ mutual Hill radii, $R_{hill,m}$ are typical. Where[1]

$$R_{hill,m} \equiv \left(\frac{M_k + M_{k+1}}{3M_*}\right)^{1/3} \frac{a_k + a_{k+1}}{2} \tag{6}$$

Here M_* is the stellar mass, M_k are the planetary masses, and a_k the semi-major axes. However, terrestrial planets that form more rapidly (i.e. before gas disk dispersal) may be more tightly-packed, as may also be the case for giant planets that necessarily form in a dissipative environment. Giant planets (or their cores) can migrate due to either planetesimal (*Levison et al.* 2010) or gas disk interactions (*Kley and Nelson* 2012). Hydrodynamic simulations of multiple planets interacting with each other and with a surrounding gas disk (*Moeckel et al.* 2008; *Marzari et al.* 2010; *Moeckel and Armitage* 2012; *Lega et al.* 2013) show that resonant, tightly packed or well-separated systems can form, but the probabilities for these channels cannot be predicted from first principles. Constraints on the dynamics must currently be derived from comparison of the predicted end states with observed systems.

For giant planets, two types of instability provide dynamical paths that may explain the origin of hot Jupiters and eccentric giant planets. If the planets start on circular, coplanar orbits, *planet-planet* scattering results in a combination of physical collisions, ejection, and generation of eccentricity. If the system instead forms with planets on widely-separated eccentric or inclined orbits, *secular chaos* can result in the diffusive evolution of eccentricity to high values even in the absence of close encounters.

[1] This is one definition of the mutual Hill radius; there are others in use in the literature.

3.1 Conditions and time scales of instability

The condition for stability can be analytically derived for two planet systems. *Gladman* (1993), drawing on results from *Marchal and Bozis* (1982) and others, showed that two planet systems with initially circular and coplanar orbits are Hill stable for separations $\Delta \equiv (a_2 - a_1)/R_{hill,m} \gtrsim 2\sqrt{3}$. Hill stability implies that two planets with at least this separation are analytically guaranteed to never experience a close approach. Numerically, it is found that some systems can be stable at smaller separations within mean motion resonances, and that the stronger condition of Lagrange stability — which requires that both planets remain bound and ordered for all time — requires only modestly greater spacing than Hill stability (*Barnes and Greenberg* 2006b; *Veras and Mustill* 2013).

There is no analytic criterion for the absolute stability of systems with $N \geq 3$ planets. The degree of instability can be characterized numerically by evaluating the time scale for orbit crossing, or for the first close encounters between planets, to occur (in practice, different reasonable definitions of "instability" are nearly equivalent). Figure 1 illustrates the median instability time scale as a function of the separation in units of $R_{hill,m}$ for planetary systems of three equal mass planets with varying mass ratios $\mu = M_p/M_*$. The behavior is simplest for low mass planets. In this regime, *Chambers et al.* (1996) found that the time before the first close encounters could be approximated as $\log(t_{close}) = b\Delta + c$, with b and c being constants. The time to a first close encounter is found to vary enormously over a small range of initial planetary separations. Systems with $N = 5$ were less stable than the $N = 3$ case, but there was little further decrease in the stability time with further increase in the planet number to $N = 10$ or $N = 20$. The scaling of the instability time with separation was found to be mass dependent if measured in units of $R_{hill,m}$ (with a steeper dependence for larger μ), but approximately *independent* if measured in units $\propto M_p^{1/4}$. *Smith and Lissauer* (2009) extended these results with longer integrations. They found that a single slope provided a good fit to their data for Earth mass planets for $3.5 \leq \Delta \leq 8$, but that there was a sharp increase in b for $\Delta > 8$. Sufficiently widely separated systems thus rapidly become stable for practical purposes. As in the two planet case, resonant systems can evade the non-resonant stability scalings, but only for a limited number of planets (*Matsumoto et al.* 2012).

Similar numerical experiments for more massive planets with $\mu \sim 10^{-3}$ were conducted by *Marzari and Weidenschilling* (2002) and by *Chatterjee et al.* (2008). At these mass ratios, the plot of $t_{close}(\Delta)$ exhibits a great deal of structure associated with the 2:1 (and to a lesser extent 3:1) mean-motion resonance (Figure 1). A simple exponential fit is no longer a good approximation for instability time scales of

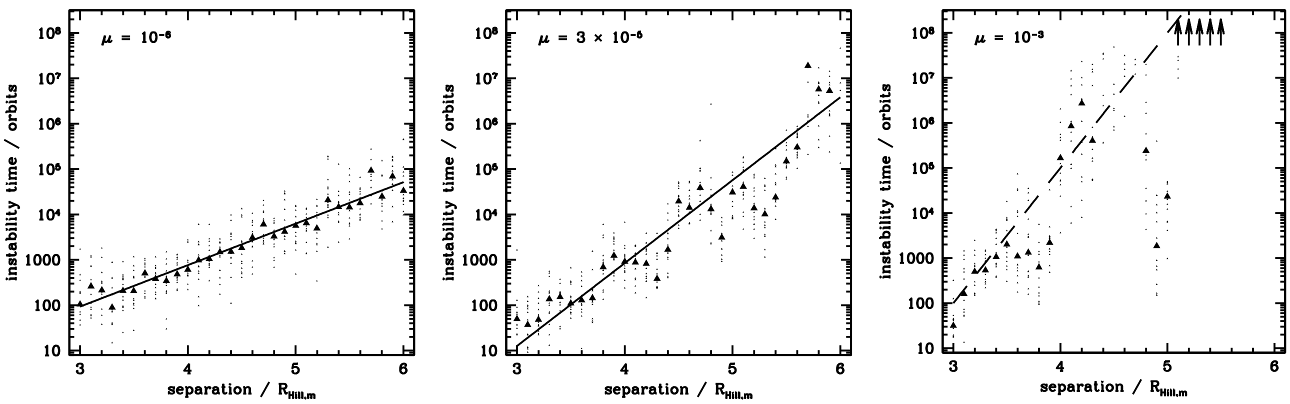

Fig. 1.— The median (triangles) instability time scale for initially circular, coplanar three planet systems, as a function of the separation in units of mutual Hill radii (after *Chambers et al.* 1996; *Marzari and Weidenschilling* 2002). The dots show the instability time scale obtained for individual realisations of a planetary system. The instability time scale is defined as the time (in units of the initial orbital period of the inner planet) until the first pair of planets approach within one Hill radius. From left to right, the panels show mass ratios $\mu = M_p/M_*$ of 10^{-6}, 3×10^{-5} and 10^{-3}.

$10^6 - 10^8$ yr (at a few AU) that might be highly relevant for gas giants emerging from the gas disk. *Chatterjee et al.* (2008) quote an improved fitting formula for the instability time (valid away from resonances), but there is an unavoidable dependence on details of the system architecture such as the radial ordering of the masses in systems with unequal mass planets (*Raymond et al.* 2010).

For a single planet, resonance overlap leads to chaos and instability of test particle orbits out to a distance that scales with planet mass as $\Delta a \propto \mu^{2/7}$ for low eccentricities (*Wisdom* 1980) and $\Delta a \propto \mu^{1/5}$ above a (small) critical eccentricity (*Mustill and Wyatt* 2012). Resonance overlap is similarly thought to underly the numerical results for the stability time of multiple planet systems (*Lissauer* 1995; *Morbidelli and Froeschlé* 1996), though the details are not fully understood. *Quillen* (2011) considered the criterion for the overlap of three-body resonances, finding that the density of these resonances was (to within an order of magnitude) sufficient to explain the origin of chaos and instability at the separations probed numerically by *Smith and Lissauer* (2009).

Once stars depart the main sequence, the increase in μ as the star loses mass can destabilize either multiple planet systems (*Duncan and Lissauer* 1998; *Debes and Sigurdsson* 2002; *Veras et al.* 2013; *Voyatzis et al.* 2013), or asteroid belts whose members are driven to encounter mean motion resonances with a single massive planet (*Debes et al.* 2012). These "late" instabilities may explain the origin of metal-polluted white dwarfs, and white dwarfs with debris disks.

3.2 Outcome of instability

The outcome of instability in tightly packed planetary systems is a combination of ejections, physical collisions between planets, and planet-star close approaches that may lead to tidal dissipation or direct collision with the star. In more widely spaced systems the same outcomes can occur, but chaotic motion can also persist indefinitely without dramatic dynamical consequences. In the inner Solar System, for example, the Lyapunov time scale is very short ($\simeq$ 5 Myr), but the only known pathway to a planetary collision — via the entry of Mercury into a secular resonance with Jupiter — has a probability of only $P \approx 10^{-2}$ within 5 Gyr (*Laskar* 1989; *Batygin and Laughlin* 2008; *Laskar and Gastineau* 2009).

During a close encounter between two planets, scattering is statistically favored over collisions when the escape speed from the planets' surfaces is larger than the escape speed from the planetary system (*Goldreich et al.* 2004). This can be quantified by the Safronov number Θ:

$$\Theta^2 = \left(\frac{M_p}{M_\star}\right)\left(\frac{R_p}{a_p}\right)^{-1} \tag{7}$$

where M_p, R_p and a_p represent the planet's mass, radius, and orbital distance, and $M_\star$ is the stellar mass (see discussion in *Ford and Rasio* 2008). We expect scattering to be most important among massive, dense planets and in the outer parts of planetary systems. In the Solar System, the giant planets' escape speeds are roughly 2-6 times larger than the highest value for the terrestrial planets (Earth's). They are also at larger a_p.

Physical collisions lead to modest eccentricities for the merged remnants (*Ford et al.* 2001). Scattering at orbital radii beyond the snow line ($a \approx 3$ AU), conversely, results in a broad eccentricity distribution consistent with that observed for massive extrasolar planets (*Chatterjee et al.* 2008; *Jurić and Tremaine* 2008). Ejection proceeds via scattering on to highly eccentric orbits, and hence a prediction of planet-planet scattering models is the existence of a population of planets around young stars with very large orbital separation (*Veras et al.* 2009; *Scharf and Menou* 2009; *Malmberg et al.* 2011). The frequency of ejections from scattering is probably too small to explain the large abundance of apparently unbound Jupiter-mass objects discovered by microlensing (*Sumi et al.* 2011), if those are to be free-floating rather than simply on wide but bound orbits (*Veras and Raymond* 2012).

The outcome of instabilities that occur within the first few Myr (or as the disk disperses) may be modified by gravitational torques or mass accretion from the protoplanetary disk, while instabilities toward the outer edges of planetary systems will result in interactions with outer planetesimal belts. *Matsumura et al.* (2010), using N-body integrations coupled to a one dimensional gas disk model, and *Moeckel and Armitage* (2012), using two dimensional hydrodynamic disk models, found that realistic transitions between gas-rich and gas-poor dynamics did not preclude the generation of high eccentricities via scattering. Larger numbers of resonant systems were, however, predicted. *Lega et al.* (2013), instead, found that if a planetary system becomes unstable during the gas-disk phase it is likely to stabilize (after the ejection or the collision of some planets) in resonant low-eccentricity orbits, and avoid further instabilities after that the gas is removed. *Raymond et al.* (2010) ran scattering experiments in which planets at larger radii interacted with massive collision-less planetesimal disks. The disks strongly suppressed the final eccentricities of lower mass outer planetary systems.

3.3 Secular chaos

Significantly different evolution is possible in multiple planet systems if one or more planets possess a substantial eccentricity or inclination from the *beginning*. The departure from circular coplanar orbits can be quantified by the angular momentum deficit (AMD) defined earlier.

Wu and Lithwick (2011) proposed secular chaos (combined with tidal effects) as the origin of hot Jupiters. They presented a proof of concept numerical integration of a widely separated (but chaotic) planetary system in which most of the AMD initially resided in an eccentric ($e \approx 0.3$) outer gas giant ($M = 1.5\ M_J$, $a = 16$ AU). Diffusion of AMD among the three planets in the system eventually led to the innermost planet attaining $e \simeq 1$ without prior close encounters among the planets. They noted several characteristic features of secular chaos as a mechanism for forming hot Jupiters — it works best for low mass inner planets, requires the presence of multiple additional planets at large radii, and can result in star-planet tidal interactions that occur very late (in principle after Gyr).

The range of planetary systems for which secular chaos yields dynamically interesting outcomes on short enough time scales remains to be quantified. A prerequisite is a large enough AMD in the initial conditions. This might originate from eccentricity excitation of planets by the gas disk (though this is unlikely to occur for low planet masses, e.g. *Papaloizou et al.* 2001; *D'Angelo et al.* 2006; *Dunhill et al.* 2013), from external perturbations such as fly-bys (*Malmberg et al.* 2011; *Boley et al.* 2012), or from a prior epoch of scattering among more tightly packed planets.

4. PLANET-PLANET SCATTERING CONSTRAINED BY DYNAMICS AND OBSERVED EXOPLANETS

The planet-planet scattering model was developed to explain the existence of hot Jupiters (*Rasio and Ford* 1996; *Weidenschilling and Marzari* 1996) and giant planets on very eccentric orbits (*Lin and Ida* 1997; *Papaloizou and Terquem* 2001; *Ford et al.* 2001). Given the great successes of exoplanet searches there now exists a database of observations against which to test the planet-planet scattering model. The relevant observational constraints come from the subset of extra-solar systems containing giant planets. In this Section we first review the relevant observational constraints. Next, we show how the dynamics of scattering depends on the parameters of the system. We then show that, with simple assumptions, the scattering model can match the observations.

4.1 Constraints from Giant Exoplanets

The sample of extra-solar planets that can directly constrain models of planet-planet scattering now numbers more than 300. These are giant planets with masses larger than Saturn's and smaller than $13 M_{Jup}$ (*Wright et al.* 2011; *Schneider et al.* 2011) with orbital semimajor axes larger than 0.2 AU to avoid contamination from star-planet tidal circularization.

The giant planets have a broad eccentricity distribution with a median of $\sim\ 0.22$ (*Butler et al.* 2006; *Udry and Santos* 2007). There are a number of planets with very eccentric orbits: roughly 16% / 6% / 1% of the sample has eccentricities larger than 0.5 / 0.7 / 0.9.

More massive planets have more eccentric orbits. Giant exoplanets with minimum masses $M_p > M_{Jup}$ have statistically higher eccentricities (as measured by a K-S test) than planets with $M_p < M_{Jup}$ (*Jones et al.* 2006; *Ribas and Miralda-Escudé* 2007; *Ford and Rasio* 2008; *Wright et al.* 2009). Excluding hot Jupiters, there is no measured correlation between orbital radius and eccentricity (*Ford and Rasio* 2008).

Additional constraints can be extracted from multiple planet systems. For example, the known two-planet systems are observed to cluster just beyond the Hill stability limit (*Barnes and Greenberg* 2006a; *Raymond et al.* 2009b). However, it's unclear to what extent detection biases contribute to this clustering. In addition, studies of the long-term dynamics of some well-characterized systems can constrain their secular behavior, and several systems have been found very close to the boundary between apsidal libration and circulation (*Ford et al.* 2005; *Barnes and Greenberg* 2006b; *Veras and Ford* 2009).

Often, there are significant uncertainties associated with the observations (*Ford* 2005). Orbital eccentricities are especially hard to pin down and the current sample may be modestly biased toward higher eccentricities (*Shen and Turner* 2008; *Zakamska et al.* 2011), although it is clear that with their near-circular orbits the Solar System's giant planets are unusual in the context of giant exoplanets.

4.2 Scattering Experiments: Effect of System Parameters

We now explore how the dynamics and outcomes of planet-planet scattering are affected by parameters of the giant planets, in particular their masses and mass ratios. Our goal is to understand what initial conditions are able to match all of the observed constraints from Section 4.1.

During a close gravitational encounter, the magnitude of the gravitational kick that a planet imparts depends on the planet's escape speed. To be more precise, what is important is the Safronov number Θ, as given in Equation (7). At a given orbital distance, more massive planets kick harder, i.e. they impart a stronger change in velocity. Within systems with a fixed number of equal-mass planets, more massive systems evolve more quickly because they require fewer close encounters to give kicks equivalent to reaching zero orbital energy and being liberated from the system. The duration of an instability – the time during which the planets' orbits cross – is thus linked to the planet masses. For example, in a set of simulations with three planets at a few to 10 AU, systems with $M_p = 3M_{Jup}$ planets underwent a median of 81 scattering events during the instability, but this number increased to 175, 542, and 1871 for $M_p = M_{Jup}, M_{Sat}$, and $30M_{\oplus}$, respectively (*Raymond et al.* 2010). The instabilities lasted $10^4 - 10^6$ years; longer for lower-mass planets.

Thus, the timescale for orbital instabilities in a system starts off longer than the planet formation timescale and decreases as planets grow their masses. The natural outcome of giant planet formation is a planetary system with multiple giant planets which undergo repeated instabilities on progressively longer timescales, until the instability time exceeds the age of the system.

The orbits of surviving planets in equal-mass systems also depend on the planet mass. Massive planets end up on orbits with larger eccentricities than less massive planets (*Ford et al.* 2003; *Raymond et al.* 2008, 2009a, 2010). This is a natural consequence of the stronger kicks delivered by more massive planets. However, the inclinations of surviving massive planets are smaller than for less massive planets in terms of both the inclination with respect to the initial orbital plane (presumably corresponding to the stellar equator) and the mutual inclination between the orbits of multiple surviving planets (*Raymond et al.* 2010). This increase in inclination appears to be intimately linked with the number of encounters the planets have experienced in ejecting other planets rather than their strength.

The planetary mass ratios also play a key role in the scattering process. Scattering between equal-mass planets represents the most energy-intensive scenario for ejection. Since it requires far less energy to eject a less massive planet, the recoil that is felt by the surviving planets is much less. Thus, the planets that survive instabilities between unequal-mass planets have smaller eccentricities and inclinations compared with the planets that survive equal-mass scattering (*Ford et al.* 2003; *Raymond et al.* 2008, 2010, 2012). This does not appear to be overly sensitive to the planets' ordering, i.e. if the lower-mass planets are located on interior or exterior orbits (*Raymond et al.* 2010).

The timing of the instability may also be important for the outcome because giant planets cool and contract on 10^{7-8} year timescales (*Spiegel and Burrows* 2012). Thus, the planets' escape speeds and Θ values increase in time. Instabilities that occur very early in planetary system histories may thus be less efficient at ejecting planets and may include a higher rate of collisions compared with most scattering calculations to date.

4.3 Scattering Experiments: Matching Observations

Let us consider a simple numerical experiment where all planetary systems containing giant planets are assumed to form three giant planets. The masses of these planets follow the observed mass distribution $\mathrm{d}N/\mathrm{d}M \propto M^{-1.1}$ (*Butler et al.* 2006; *Udry and Santos* 2007) and the masses within a system are not correlated. All systems become unstable and undergo planet-planet scattering. With no fine tuning, the outcome of this experiment matches the observed eccentricity distribution (*Raymond et al.* 2008).

The exoplanet eccentricity distribution can be reproduced with a wide range of initial conditions (*Adams and Laughlin* 2003; *Moorhead and Adams* 2005; *Jurić and Tremaine* 2008; *Chatterjee et al.* 2008; *Ford and Rasio* 2008; *Raymond et al.* 2010; *Beaugé and Nesvorný* 2012). The same simulations also reproduce the dynamical quantities that can be inferred from multiple-planet systems: the distribution of parameterized distances of two-planet systems from the Hill stability limit (*Raymond et al.* 2009b) and the secular configuration of two-planet systems (*Timpe et al.* 2012).

Certain observations are difficult to reproduce. Some observed systems show no evidence of having undergone an instability (e.g. as they contain multiple giant planets on near-circular orbits or those in resonances). The scattering model must thus be able to reproduce the observed distributions including a fraction of systems remaining on stable orbits. The fraction of systems that are stable is typically 10-30%, where assumptions are made about the distribution of planetary masses and orbits (*Jurić and Tremaine* 2008; *Raymond et al.* 2010, 2011). One should also note that migration is required in order to match the observed distribution of semi-major axes, in other words scattering alone cannot transport Jupiter-like planets on Jupiter-like orbits to semi-major axes less than one AU (*Moorhead and Adams* 2005).

Perhaps the most difficult observation to match is the observed positive correlation between planet mass and eccentricity. In the simulations from the simple experiment mentioned above, lower-mass surviving planets actually have higher eccentricities than more massive ones (*Raymond et al.* 2010). For massive planets to have higher eccentricities they must form in systems with other massive planets, since scattering among equal-mass massive planets produces the highest eccentricities. This is in agreement with planet formation models: when the conditions are ripe for giant planet formation (e.g. massive disk, high metallicity), one would expect all giants to have high masses, and vice versa.

It is relatively simple to construct a population of systems that can reproduce the observed eccentricity distribution as well as the mass-eccentricity correlation and also the mass distribution. The population consists of equal-mass high-mass systems and a diversity of lower-mass systems that can include unequal-mass systems or equal-mass ones. This population also naturally reproduces the observed distribution of two-planet systems which pile up close to the Hill stability limit (as shown in Figure 2).

We conclude this section with a note of caution. Given the observational uncertainties and the long list of system parameters, to what degree can our understanding of planet-planet scattering constrain pre-instability planetary systems? The scattering mechanism is robust and can reproduce observations for a range of initial conditions. Beyond the limitations of mass, energy and angular momentum conservation, the details of pre-scattered systems remain largely hidden from our view. The only constraint that appears to require correlated initial conditions to solve is the mass-eccentricity correlation.

Finally, planet-planet scattering does not happen in isolation but rather affects the other components of planetary systems. Giant planet instabilities are generally destructive to both inner rocky planets (*Veras and Armitage* 2005, 2006; *Raymond et al.* 2011, 2012; *Matsumura et al.* 2013) and to outer planetesimal disks (*Raymond et al.* 2011, 2012; *Raymond and Armitage* 2013). Additional constraints on giant planet dynamics may thus be found in a number of places. Recent discoveries by the Kepler Mission of Earth and super-Earth-size planets relatively close to their host star reveal only a small fraction with giant planets orbiting nearby (*Lissauer et al.* 2011; *Ciardi et al.* 2013). Multiple systems also appear to be rather flat and stable to planet-planet interactions (*Lissauer et al.* 2011; *Tremaine and Dong* 2012; *Johansen et al.* 2012; *Fang and Margot* 2012a).

Characterizing the relationship between small planets orbiting close to the host star and more massive planets at larger separations could provide insights into the effects of planet scattering on the formation of inner, rocky planets. Similarly, the abundance and mass distribution of planets with large orbital separations (*Malmberg et al.* 2011; *Boley et al.* 2012) or free-floating planets may provide insights into the planets that are scattered to the outskirts of planetary systems or into the galaxy as free-floating planets (*Veras and Ford* 2009; *Veras et al.* 2011; *Veras and Raymond* 2012; *Veras and Mustill* 2013). In addition, the fact that planet-planet scattering perturbs both the inner and outer parts of planetary systems may introduce a natural correlation between the presence of debris disks and close-in low-mass planets, as well as an anti-correlation between debris disks and eccentric giant planets (*Raymond et al.* 2011, 2012; *Raymond and Armitage* 2013).

5. PLANETS AND PLANETESIMAL DISKS

This section considers the evolution of planetary orbits due to interactions with planetesimal disks. These disks are likely to remain intact after the gaseous portion of the disk has gone away, i.e., for system ages greater than 3–10 Myr, and will continue to evolve in time. Such planetesimal disks are likely to be most effective during the subsequent decade of time, for system ages in the range 10–100 Myr. One of the main effects of a residual planetesimal disk is to drive planetary migration. The subsequent changes in the orbital elements of the planets can cause instabilities (e.g. induced by resonance crossing or by the extraction of the planets from their original resonances), and such action can drive orbital eccentricities to larger values. On the other hand, planetesimal disks can also damp orbital eccentricity and thereby act to stabilize planetary systems.

We begin with a brief overview of the basic properties of planetismal disks. Unfortunately, we cannot observe planetesimal disks directly. Instead, we can piece together an understanding of their properties by considering protoplanetary disks around newly formed stars (see the review of *Williams and Cieza* 2011) and debris disks (see the reviews of *Zuckerman* 2001; *Wyatt* 2008). These latter systems represent the late stages of circumstellar disk evolution, after the gas has been removed, either by photoevaporation or by accretion onto the central star (see the chapter by *Alexander et al.* for more details of the photoevaporation process).

Most of the observational information that we have concerning both types of disks is found through their spectral energy distributions (SEDs), especially the radiation emitted at infrared wavelengths. Since these SEDs are primarily sensitive to dust grains, rather than the large planetesimals of interest here, much of our information is indirect. The defining characteristic of debris disks is their fractional luminosity f, essentially the ratio of power emitted at infrared wavelengths to the total power of the star itself. True debris disks are defined to have $f < 10^{-2}$ (*Lagrange et al.* 2000), whereas systems with larger values of f are considered to be protoplanetary disks. For both types of systems, the observed fluxes can be used to make disk mass estimates. The results show that the disk masses decrease steadily with time. For young systems with ages ~ 1 Myr, the masses in solid material are typically $M_d \sim 100 M_\oplus$, albeit with substantial scatter about this value. Note that this amount of solid material is not unlike that of the Minimum Mass Solar/Extrasolar Nebula (e.g. *Weidenschilling* 1977; *Kuchner* 2004; *Chiang and Laughlin* 2013). By the time these systems reach ages of ~ 100 Myr, in the inner

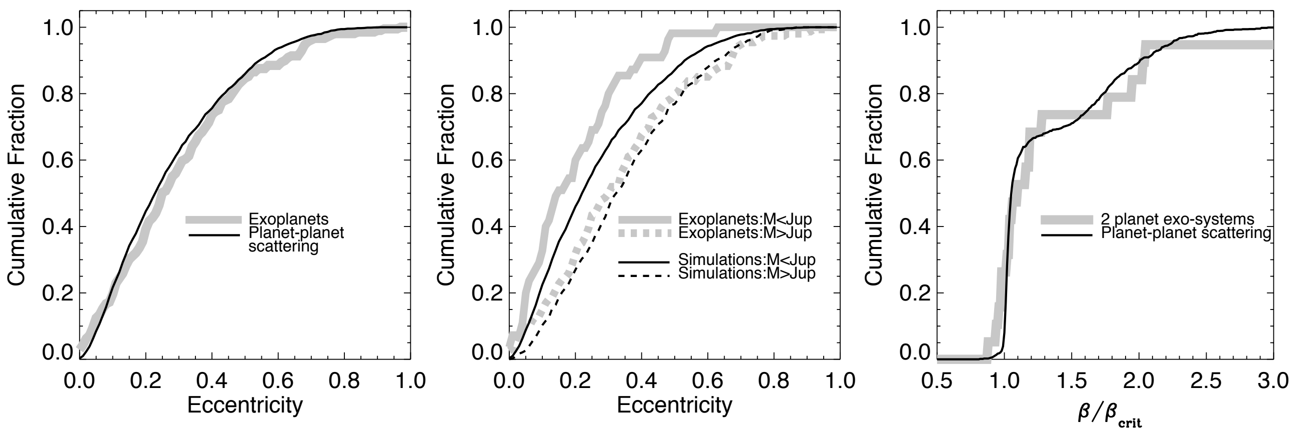

Fig. 2.— A comparison between observed properties of giant exoplanets (shown in gray) and planet-planet scattering simulations (in black). Left: the eccentricity distribution. Middle: the eccentricity distribution for low-mass (dashed curves) and high-mass (solid curves) planets. Right: The proximity to the Hill stability limit, measured by the quantity β/β_{crit} (*Barnes and Greenberg* 2006b; *Raymond et al.* 2009b) where the stability limit occurs at $\beta/\beta_{crit} = 1$ and systems with larger values of β/β_{crit} are stable.

part of the disk the masses have fallen to only $\sim 0.01 M_\oplus$ (see Figure 3 of *Wyatt* 2008). Note that these mass estimates correspond to the material that is contained in small dust grains; some fraction of the original material is thought to be locked up in larger bodies – the planetesimals of interest here. As a result, the total mass of the planetesimal disk does not necessarily fall as rapidly with time as the SEDs suggest.

At large distances from the star, instead, the decay of the mass of the dust population is much slower, suggesting that belts containing tens of Earth masses can exist around Gyr-old stars (*Booth et al.* 2009).

For a given mass contained in the planetesimal disk, we expect the surface density of solid material to initially follow a power-law form so that $\sigma \propto r^{-p}$, where the index p typically falls in the approximate range $1/2 \leq p \leq 2$ (*Cassen and Moosman* 1981). The disks are initially expected to have inner edges where the protoplanetary disks are truncated by magnetic fields, where this boundary occurs at $r \sim 0.05$ AU. Similarly, the outer boundaries are initially set by disk formation considerations. The angular momentum barrier during protostellar collapse implies that disks start with outer radii $r_d \sim 10 - 100$ AU (*Cassen and Moosman* 1981; *Adams and Shu* 1986). Further environmental sculpting of disks (see Section 6 below) reinforces this outer boundary. The properties outlined here apply primarily to the starting configurations of the planetesimal disks. As the disks evolve, and interact with planets, the surface density must change accordingly.

Given the properties of planetesimal disks, we now consider how they interact with planets and drive planetary migration. The physical mechanism by which planetesimals lead to planet migration can be roughly described as follows (see, e.g., *Levison et al.* 2007): Within the disk, as the planetesimals gravitationally scatter off the planet, the larger body must recoil and thereby change its trajectory. Since the planet resides within a veritable sea of planetesimals, the smaller bodies approach the larger body from all directions, so that the momentum impulses felt by the planet are randomly oriented. As a result, the orbital elements of the planet will experience a random walk through parameter space. In particular, the semi-major axis of the planetary orbit will undergo a random walk. If the random walk is perfectly symmetric, then the planet has equal probability of migrating inward or outward; nonetheless, changes will accumulate (proportional to the square root of the number of scattering events). In practice, however, many factors break the symmetry (e.g., the surface density of solids generally decreases with radius) and one direction is preferred.

The details of planetary migration by planetesimal disks depend on the specific properties of the planetary system, including the number of planets, the planet masses, their separations, the radial extent of the disk, and of course the total mass in planetesimals. In spite of these complications, we can identify some general principles that guide the evolution. Some of these are outlined below:

We first note that a disk of planetesimals containing planets often evolves in what can be called a “diffusive regime”, where many small scattering events act to make the orbital elements of both the planets and the planetesimals undergo a random walk. As a result, the system has the tendency to spread out. This behavior is often seen in numerical simulations. For a system consisting of a disk of planetesimals and analogs of the four giant planets in our Solar System, the scattering events in general lead to Jupiter migrating inward and the remaining three planets migrating outward (*Fernandez and Ip* 1984; *Hahn and Malhotra* 1999; *Gomes et al.* 2004) Similarly, in numerical simula-

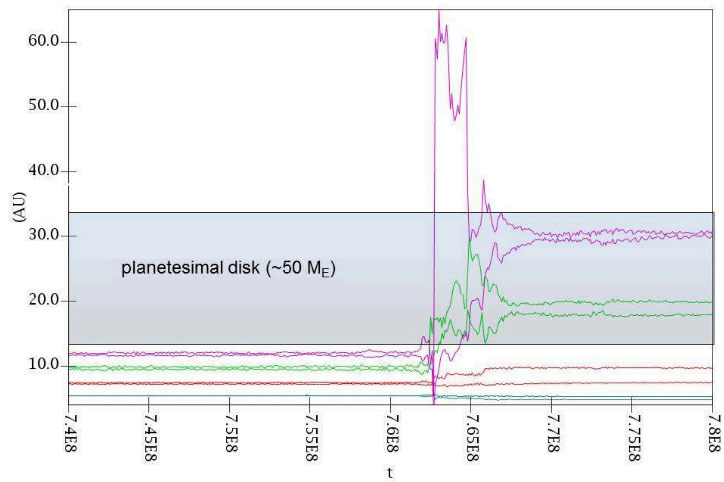

Fig. 3.— Orbital evolution of the four giant planets in our Solar System according to the Nice model. Here, each planet is represented by two curves, denoting perihelion and aphelion distance. Hence, when the curves overlap the orbit is circular. The region spanned originally by the planetesimal disk of 50 Earth masses is shown as a grey area. Notice that the planetary system becomes unstable at $t = 762$ Myr in this simulation with the planetary orbits changing radically at this point (data from *Levison et al.* 2011).

tions of systems with two planets embedded in a disk of planetesimals, the inner planet often migrates inward, while the outer planet migrates outward (*Levison et al.* 2007). Instead, a single planet in a planetesimal disk, in general migrates inwards (*Kirsh et al.* 2009). This can be understood using some considerations concerning energy conservation. For a system made of a planet and a disk of planetesimals energy is conserved until planetesimals are lost. Planetesimals can be lost by collisions with the planet, collisions with the Sun or ejection onto hyperbolic orbit. In the case where the latter is the major loss mechanism, which happens if the planet is massive and the disk is dynamically excited, the removed planetesimals subtract energy to the system of bodies remaining in orbit around the star. Consequently, most of the mass has to move inward and the planet has to follow this trend. Given the expected total masses in planetesimals (see the above discussion), this mode of migration cannot change the semimajor axis of a planetary orbit by a large factor. In particular, this mechanism is unlikely to produce Hot Jupiters with periods of about four days and therefore these planets have to form by a different mechanism (migration in a disk of gas or planet-planet scattering and tidal damping).

Finally, we note that the effects discussed above can be modified in the early phases of evolution by the presence of a gaseous component to the disk (*Capobianco et al.* 2011). For instance, planetesimals scattered inwards by the planet may have their orbits circularized by gas drag, so that they cannot be scattered again by the planet. Consequently, the trend is that the planetesimal population loses energy and the planet has to migrate outwards.

Planetary migration enforced by the scattering of planetesimals will produce a back reaction on the disk. As outlined above, the disk will tend to spread out, and some planetesimals are lost by being scattered out of the system. Both of these effects reduce the surface density in planetesimals. In addition, the planets can create gaps in the disk of planetesimals. These processes are important because they are potentially observable with the next generation of interferometers (ALMA). We note, however, that submillimeter (and millimeter wave) observations are primarily sensitive to dust grains rather than planetesimals themselves. The stirring of the planetesimal disk by planets can lead to planetesimal collisions and dust production, thereby allowing these processes to be observed.

Since planetesimal disks are likely to be present in most systems, it is interesting to consider what might have occurred in the early evolution of our own Solar System. Here we follow the description provided by the so-called “Nice model”. As described in Section 2, it is expected that, at the end of the gas-disk phase, the giant planets were in a chain of resonant (or nearly resonant) orbits, with small eccentricities and inclinations, and narrow mutual separations. These orbital configurations are those that are found to reach a steady-state, and hence are used as the initial condition for the Nice model (*Morbidelli et al.* 2007). The model also assumes that beyond the orbit of Neptune there was a planetesimal disk, carrying cumulatively approximately 30-50 Earth masses. A disk in this mass range is necessary to allow the giant planets to evolve from their original, compact configuration to the orbits they have today. More specifically, the perturbations between the planets and this disk, although weak, accumulated over time and eventually extracted a pair of planets from their resonance. The breaking of the resonance lock makes the planetary system unstable. After leaving resonance, the planets behave as described in Sections 3 and 4, and as shown in Figure 3. Their mutual close encounters act to spread out the planetary system and to excite the orbital eccentricities and inclinations. In particular, this model suggests that Uranus and Neptune got scattered outwards by Jupiter and Saturn, penetrated into the original trans-Neptunian disk and dispersed it. The dispersal of the planetesimal disk, in turn, damped the orbital eccentricities of Uranus and Neptune (and to a lesser extent those of Jupiter and Saturn), so that the four giant planets eventually reached orbits analogous to the current ones (*Morbidelli et al.* 2007; *Batygin and Brown* 2010; *Batygin et al.* 2012; *Nesvorný and Morbidelli* 2012).

In addition to the current orbits of the giant planets, the Nice model accounts for the properties of the small body populations which, as we described in Section 3, suggest that the structure of the solar system experienced dramatic changes after gas dissipation. In fact, the model has been shown to explain the structure of the Kuiper belt (*Levison et al.* 2008; *Batygin et al.* 2011), the asteroid belt (*Morbidelli et al.* 2010), and even the origin of the Oort cloud (*Brasser and Morbidelli* 2013). Moreover, it has been shown that, with reasonable assumptions concerning the planetesimal disk, the instability of the planetary orbits could occur after hundreds of Myr of apparent stability (*Tsiganis et al.* 2005; *Gomes et al.* 2005; *Levison et al.* 2011); the subsequent epoch of instability could excite the orbits of the small bodies and thereby produce a shower of projectiles into the inner solar system that quantitatively explains the origin of the Late Heavy Bombardment (*Bottke et al.* 2012).

At the present time, there are no gross characteristics of the Solar System that are at odds with the Nice model. Nevertheless, some aspects of the general picture associated with the model need to be revised or explored. For instance, the cold population (which is a sub-population of the Kuiper belt characterized by small orbital inclinations) probably formed in-situ (*Parker and Quanz* 2012) instead of being implanted from within $\sim$ 30 AU as envisioned in *Levison et al.* (2008). Also, *Nesvorný and Morbidelli* (2012) showed that the current orbits of the planets are better reproduced if one postulates the existence of a fifth planet with a mass comparable to those of Uranus and Neptune, eventually ejected from the Solar System. However, it has not yet been shown that a 5-planet system can become unstable late, the work of *Levison et al.* (2011) having been conducted in the framework of a 4-planet system. These issues, however, are unlikely to invalidate the Nice model as a whole.

It may be surprising that the current eccentricities and inclinations of the giant planets of our solar system can be so much smaller than those of many extra-solar planets, especially if they experienced a similar phase of global instability (see Sections 3 and 4). There are two main reasons for this result. First, the "giant" planets of our solar system have masses that are significantly smaller than those of many extra-solar giant planets. This lower (total) mass made the instability less violent and allowed the orbits of our giant planets to be damped more efficiently by interactions with the planetesimal disk (*Raymond et al.* 2009a). This trend is particularly appplicable for Uranus and Neptune: Their eccentricities could be damped from more than 0.5 to almost zero by the dispersal of the planetesimal disk, which is assumed to carry about twice the sum of their masses. Second, Jupiter and Saturn fortuitously avoided having close encounters with each other (whereas they both had, according to the Nice model, encounters with a Neptune-mass planet). In fact, in the simulations of solar system instability where Jupiter and Saturn have a close encounter with each other, Jupiter typically ends up on an orbit with eccentricity in the range $e = 0.3 - 0.4$ (typical of many extra-solar planets) and recoils to 4.5 AU, while all of the other planets are ejected from the system.

6. DYNAMICAL INTERACTIONS OF PLANETARY SYSTEMS WITHIN STELLAR CLUSTERS

In this section we consider dynamical interactions between the constituent members of young stellar clusters with a focus on the consequent effects on young and forming planetary systems.

Most stars form within some type of cluster or association. In order to quantify the resulting effects on planetary systems, we first consider the basic properties of these cluster environments. About 10 percent of the stellar population is born within clusters that are sufficiently robust to become open clusters, which live for 100 Myr to 1 Gyr. The remaining 90 percent of the stellar population is born within shorter-lived cluster systems that we call embedded clusters. Embedded clusters become unbound and fall apart when residual gas is ejected through the effects of stellar winds and/or supernovae. This dispersal occurs on a timescale of ~ 10 Myr.

Open clusters span a wide range of masses, or, equivalently, number of members. To leading order, the cluster distribution function $f_{cl} \sim 1/N^2$ over a range from N = 1 (single stars) to $N = 10^6$ (this law requires combining data from different sources, e.g., *Lada and Lada* 2003; *Chandar et al.* 1999). With this distribution, the probability that a star is born within a cluster of size N scales as $P = N f_{cl} \sim 1/N$, so that the cumulative probability $\propto \log N$. In other words, stars are equally likely to be born within clusters in each decade of stellar membership size N. For the lower end of the range, clusters have radii of order R = 1pc, and the cluster radius scales as $R \approx 1\mathrm{pc}(N/300)^{1/2}$, so that the clusters have (approximately) constant column density (*Lada and Lada* 2003; *Adams et al.* 2006). For the upper end of the range, this law tends to saturate, so that the more-massive clusters are denser than expected from this law. Nonetheless, a typical mean density is only about 100 stars/pc^3. Clusters having typical masses and radii have velocity dispersions ~ 1 km/s.

Dynamical interactions within clusters are often subject to gravitational focussing. In rough terms, focusing becomes important when the encounter distance is small enough that the speed of one body is affected by the potential well of the other body. For a typical velocity dispersion of 1 km/s, and for solar-type stars, this critical distance is about 1000 AU. As outlined below, this distance is comparable to the closest expected encounter distance for typical clusters. As a result, gravitational focusing is important – but not dominant – in these systems.

The timescale for a given star to undergo a close encounter (where gravitational focusing is important) with another star within a distance r_{min} can be approximated by (*Binney and Tremaine* 1987)

$$\tau_{enc} \simeq 3.3 \times 10^7 \mathrm{yr} \left(\frac{100 \ \mathrm{pc}^{-3}}{n} \right) \left(\frac{v_\infty}{1 \ \mathrm{km/s}} \right) \times \left(\frac{10^3 \ \mathrm{AU}}{r_{min}} \right) \left(\frac{\mathrm{M}_\odot}{M} \right) \tag{8}$$

Here n is the stellar number density in the cluster, v_∞ is the mean relative speed at infinity of the stars in the cluster, r_{min} is the encounter distance, and M is the total mass of the stars involved in the encounter. The effect of gravitational focussing is included in the above equation.

The estimate suggested above is verified by numerical N-body calculations, which determine a distribution of close encounters (e.g., *Adams et al.* 2006; *Malmberg et al.* 2007b; *Proszkow and Adams* 2009). These studies show that the distribution has a power-law form so that the rate Γ at which a given star encounters other cluster members at a distance of closest approach less than b has the form $\Gamma = \Gamma_0 (b/b_0)^\gamma$, where (Γ_0, γ) are constants and b_0 is a fiducial value. The index $\gamma < 2$ is due to gravitational focusing. Typical encounter rates are shown in Figure 4 for clusters with N = 100, 300, and 1000 members. With this power-law form for the distribution, the expectation value for the closest encounter experienced over a 10 Myr time span is about $\langle b \rangle \approx 1000$ AU. The initial conditions in a cluster can have an important effect on the subsequent encounter rates. In particular, sub-virial clusters which contain significant substructure (i.e., lumps) will have higher encounter rates (*Allison et al.* 2009; *Parker and Quanz* 2012, see also Figure 4).

Planetary systems are affected by passing stars and binaries in a variety of ways (e.g., *Laughlin and Adams* 1998; *Adams and Laughlin* 2001; *Bonnell et al.* 2001; *Davies and Sigurdsson* 2001; *Adams et al.* 2006; *Malmberg et al.* 2007b; *Malmberg and Davies* 2009; *Spurzem et al.* 2009; *Malmberg et al.* 2011; *Hao et al.* 2013). Sufficiently close encounters can eject planets, although the cross sections for direct ejections are relatively small and can be written in the form (from *Adams et al.* 2006):

$$\Sigma_{ej} \approx 1350 (\mathrm{AU})^2 \left(\frac{M_*}{1 \mathrm{M}_\odot} \right)^{-1/2} \left(\frac{a_p}{1 \mathrm{AU}} \right) \tag{9}$$

where M_* is the mass of the planet-hosting star and a_p is the (starting) semimajor axis of the planet. Note that the

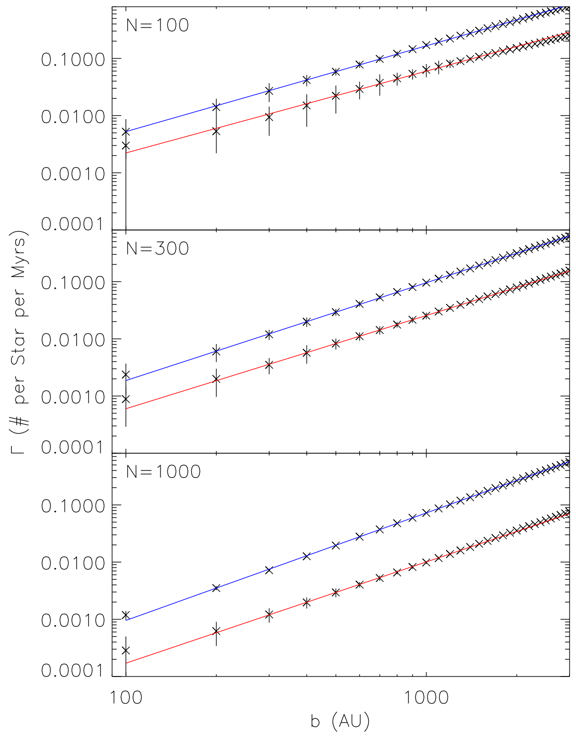

Fig. 4.— Distribution of closest approaches for the solar systems in young embedded clusters. Each panel shows the distribution of closest approaches, plotted versus approach distance b, for clusters with both virial (bottom) and sub-virial (top) starting conditions. Results are shown for clusters with N = 100, 300, and 1000 members, as labeled. The error bars shown represent the standard deviation over the compilations (Figure 5 of *Adams et al.* 2006, reproduced by permission of the AAS).

cross section scales as one power of a_p (instead of two) due to gravitational focusing.

Note that Equation (9) provides the cross section for direct ejection, where the planet in question leaves its star immediately after (or during) the encounter. Another class of encounters leads to indirect ejection. In this latter case, the fly-by event perturbs the orbits of planets in a multiple planet system, and planetary interactions later lead to the ejection of a planet. Typical instability timescales lie in the range 1 – 100 Myr (e.g., *Malmberg et al.* 2011, see their Figure 7), although a much wider range is possible. On a similar note, ejection of Earth from our own Solar System is more likely to occur indirectly through perturbations of Jupiter's orbit (so that Jupiter eventually drives the ejection of Earth), rather than via direct ejection from a passing star (*Laughlin and Adams* 2000). Planetary systems residing in wide stellar binaries in the field of the Galaxy are also vulnerable to external perturbations. Passing stars and the Galactic tidal field can change the stellar orbits of wide binaries, making them eccentric, leading to strong interactions with planetary systems (*Kaib et al.* 2013).

Although direct planetary ejections due to stellar encounters are relatively rare, such interactions can nonetheless perturb planetary orbits, i.e., these encounters can change the orbital elements of planets. Both the eccentricity and the inclination angles can be perturbed substantially, and changes in these quantities are well correlated (*Adams and Laughlin* 2001) As one benchmark, the cross section for doubling the eccentricity of Neptune in our solar system is about $\Sigma \approx (400\ \mathrm{AU})^2$; the cross section for increasing the spread of inclination angles in our solar system to 3.5 degrees has a similar value. Note that these cross sections are much larger than the geometric cross sections of the Solar System. The semi-major axes are also altered, but generally suffer smaller changes in a relative sense, i.e., $(\Delta a)/a \ll (\Delta e)/e$.

Some time after fly-by encounters, the orbital elements of planetary systems can be altered significantly due to the subsequent planet-planet interactions (see Figure 10 from *Malmberg et al.* 2011). When a planetary system becomes unstable, planets may be ejected via scattering with other planets. However, planets are often ejected as the result of several (many tens to one hundred) scattering events, with each scattering event making the planet slightly less bound to the host star. As a result, snapshots of planetary systems taken some time after the initial fly-by sometimes reveal planets on much wider (less bound) orbits with separations in excess of 100 AU. In Figure 5 we plot the fraction of post-fly-by systems containing planets on orbits with semi-major axes $a > 100$ AU as a function of time after the fly-by encounters. This trend is found both in systems made unstable by fly-bys and those that become unstable without external influence, as described earlier in Section 3 (*Scharf and Menou* 2009; *Veras et al.* 2009).

Planets on such wide orbits should be detectable via direct imaging campaigns; thus the fraction of stars possessing them will place limits on the population of unstable planetary systems.

During fly-by encounters, intruding stars can also pick up planets from the planetary system (see Figure 12 of *Malmberg et al.* 2011). Clusters thus provide rich environments that can shape the planetary systems forming within them. In particular, if the intruding star already possesses its own planetary system, the addition of the extra planet may destabilize the system.

By combining encounter rates for planetary systems in clusters with cross sections that describe the various channels of disruption, we can estimate the probability (equivalently, the perturbation rate) that a planetary system will suffer, e.g., the ejection of at least one planet over a given time interval (see *Laughlin and Adams* 1998; *Malmberg et al.* 2011). By combining the cross section for planetary ejection with the encounter histories found through N-body simulations of stellar clusters, one finds that planets will be ejected in approximately five to ten percent of planetary systems in long-lived clusters (*Malmberg et al.* 2011). The number of planets ejected directly during fly-bys will be somewhat lower: For example, only a few planets are expected to be ejected per (young) embedded cluster. As a result, large numbers of free-floating planets in young clusters point to other mechanisms for ejection, most likely planet-planet interactions in young planetary systems (*Moorhead and Adams* 2005; *Chatterjee et al.* 2008). One should also note that dynamical mechanisms are unlikely to be able to explain the population of free-floating planets as inferred by micro-lensing observations (*Veras and Raymond* 2012).

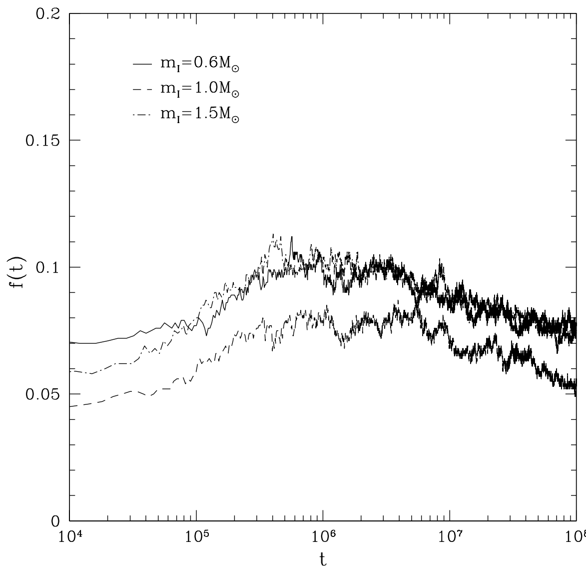

Fig. 5.— The fraction of solar systems $f(t)$ containing planets with semi-major axes greater than 100 AU, plotted here as a function of time t after a close encounter for intruder stars of masses 0.6, 1.0 and 1.5 $M_\odot$. These simulations of fly-bys involve the four gas giants of the solar system with $r_{\rm min} < 100$ AU (Figure 11 of *Malmberg et al.* 2011, reproduced by permission of RAS).

Encounters involving binary stars also play an important role in the evolution of planetary systems residing in stellar clusters. A star that hosts a planetary system may exchange into a (wide) binary. If its orbit is sufficiently inclined, the stellar companion can affect planetary orbits via the Kozai mechanism (see also Section 7). These interactions force planets onto eccentric orbits that can cross the orbits of other planets, and can thereby result in strong planetary scatterings (*Malmberg et al.* 2007a). The rate of such encounters depends on the binary population, but Kozai-induced scattering may account for the destruction of at least a few percent of planetary systems in clusters (*Malmberg et al.* 2007b).

For completeness, we note that dynamical interactions can also affect circumstellar disks, prior to the formation of planetary systems. In this earlier phase of evolution, the disks are subject to truncation by passing stars. As a general rule, the disks are truncated to about one third of the distance of closest approach (*Ostriker* 1994; *Heller*

1995); with the expected distribution of interaction distances, we expect disks to be typically truncated to about 300 AU through this process, although closer encounters will lead to smaller disks around a subset of stars. Since most planet formation takes place at radii smaller than 300 AU, these interactions have only a modest effect. In a similar vein, circumstellar disks can sweep up ambient gas in the clusters through Bondi-Hoyle accretion. Under favorable conditions, a disk can gain a mass equivalent to the minimum mass solar nebula through this mechanism (*Throop and Bally* 2008).

The orientations of circumstellar disks can also be altered by later accretion of material on the disks and by interactions with other stars within clustered environments (*Bate et al.* 2010). Alternatively, interactions with a companion star within a binary can also re-orient a disk (*Batygin* 2012). Both processes represent an alternative to the dynamical processes described in Sections 7 and 8 as a way to produce hot Jupiters on highly-inclined orbits.

Since clusters have significant effects on the solar systems forming within them, and since our own Solar System is likely to have formed within a cluster, one can use these ideas to constrain the birth environment of the Sun (*Adams* 2010). Our Solar System has been only moderately perturbed via dynamical interactions, which implies that our birth cluster was not overly destructive. On the other hand, a close encounter with another star (or binary) may be necessary to explain the observed edge of the Kuiper belt and the orbit of the dwarf planet Sedna (*Kobayashi and Ida* 2001; *Kenyon and Bromley* 2004; *Morbidelli and Levison* 2004), and the need for such an encounter implies an interactive environment. Note that the expected timescale for an encounter (about 2000 yr) is much longer than the orbital period at the edge of the Kuiper belt (350 yr), so that the edge can become well-defined. Adding to the picture, meteoritic evidence suggests that the early Solar System was enriched in short-lived radioactive isotopes by a supernova explosion (*Wadhwa et al.* 2007), an AGB star (*Wasserburg et al.* 2006), or some combination of many supernovae and a second generation massive star (*Gounelle and Meynet* 2012; *Gounelle et al.* 2013). Taken together, these constraints jointly imply that the birth cluster of the Solar System was moderately large, with stellar membership size $N = 10^3 - 10^4$ (e.g., *Hester et al.* 2004; *Adams* 2010).

7. THE LIDOV-KOZAI MECHANISM

The perturbing effect of Jupiter on the orbits of asteroids around the sun was considered by *Kozai* (1962). It was found that for sufficiently highly-inclined orbits, the asteroid would undergo large, periodic, changes in both eccentricity and inclination. Work by *Lidov* (1962) showed that similar effects could be seen for an artificial satellite orbiting a planet. Here we will refer to such perturbations as the Lidov-Kozai mechanism when also applied to perturbations of planetary orbits due to an inclined stellar compan-

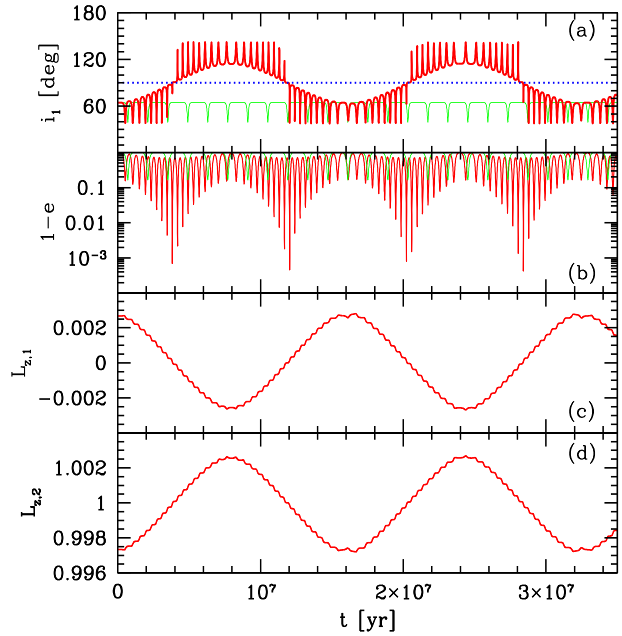

Fig. 6.— Inclination flipping due to the Lidov-Kozai mechanism when the disturbing function is truncated to octupole order (upper curve on panel a and lower curve on panel b) versus quadrupole order (lower curve on panel a and upper curve on panel b). The inner binary consists of a $1M_\odot$ star and a $1M_J$ planet separated by 6 au with $e_{\rm in} = 0.001$, and the outer body is a brown dwarf of $40M_J$ at a distance of 100 au from the center of mass of the inner binary with $e_{\rm out} = 0.6$. The bottom two plots display the normalized vertical components of the inner and outer orbit angular momentum (Figure 1 of *Naoz et al.* 2011, reprinted by permission from Macmillan Publishers Ltd: Nature, 473, 187-189, copyright 2011).

ion. Strong periodic interactions can also occur between two planets, when one is highly-inclined.

The Lidov-Kozai mechanism is a possible formation channel for hot Jupiters (as will be discussed in Section 8, *Fabrycky and Tremaine* 2007; *Nagasawa et al.* 2008). Concurrently, the Lidov-Kozai mechanism has found wide applicability to other astrophysical problems: binary supermassive black holes (*Blaes et al.* 2002); binary minor planets (where the Sun is considered the massive outer perturber) (*Perets and Naoz* 2009; *Fang and Margot* 2012b); binary millisecond pulsars (*Gopakumar et al.* 2009); stellar disc-induced Lidov-Kozai oscillations in the Galactic center (*Chang* 2009); binary white dwarfs or binary neutron stars (*Thompson* 2011); and evolving triple star systems with mass loss (*Shappee and Thompson* 2013).

Lidov-Kozai evolution is approximated analytically by applying Lagrange's Planetary Equations to a truncated and averaged form of the disturbing function (*Valtonen and Karttunen* 2006, Chapter 9). The truncation is justified because of the hierarchical ordering of the mutual distances of the three

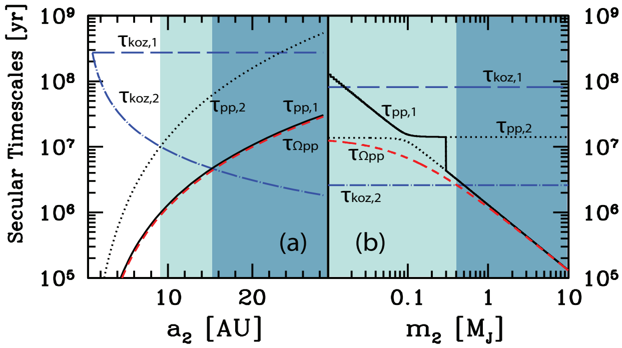

Fig. 7.— Comparison of timescales and regimes of motion for a four-body system consisting of two planets secularly orbiting one star of a wide binary. The binary separation and eccentricity are fixed at 500 AU and 0.5 for two 1M$_\odot$ stars, and the inner $0.3M_J$ planet resides 1 au away from its parent star. Subscripts of "1" and "2" refer to the inner and outer planet, "koz" the Lidov-Kozai characteristic timescale due to the distant star, and "pp" timescales due to Laplace-Lagrange secular theory. The unshaded, lightly-shaded and darkly-shaded regions refer to where Lidov-Kozai cycles on the outer planet are suppressed, the planetary orbits precess in concert, and the inner planet's eccentricity grows chaotically (Figure 14 of *Takeda et al.* 2008, reproduced by permission of the AAS).

bodies. The averaging occurs twice, over a longitude or anomaly of both the lightest body and the outermost body.

Traditionally, the disturbing function is secular, meaning that the planetary semimajor axes remain fixed and the system is free from the influence of mean motion resonances. The term "Lidov-Kozai resonance" refers simply to the Lidov-Kozai mechanism, which includes large and periodic secular eccentricity and inclination variations. Confusingly, an alteration of this mechanism that introduced non-secular contributions (*Kozai* 1985) has been referred to as a Lidov-Kozai resonance *within* a mean motion resonance. This formalism has been utilized to help model dynamics in the Kuiper Belt (*Gallardo* 2006; *Wan and Huang* 2007; *Gallardo et al.* 2012). The Lidov-Kozai mechanism can also be modified by including the effects of star-planet tides (see Section 8) resulting in significant changes in the semi-major axis of a planet (a process sometimes known as "Lidov-Kozai migration") (*Wu and Murray* 2003).

The complete analytic solution to the secular equations resulting from the truncated and averaged disturbing function may be expressed in terms of elliptic functions (*Vashkov'yak* 1999). However, more commonly an approximate solution is found for small initial values of eccentricities (e) (but where initial values of inclination (i) are sufficiently large for Lidov-Kozai cycles to occur) by truncating the disturbing function to quadrupole order in the mutual distances between the bodies. This solution demonstrates that the argument of pericenter oscillates around $90°$ or $270°$, a dynamical signature of the Lidov-Kozai mechanism. The solution also yields a useful relation: $\sqrt{1-e^2}\cos i \approx \mathrm{constant}$ subject to $i > \arcsin(2/5)$ and $e < \sqrt{1-(5/3)\cos^2(i)}$. This relation demonstrates the interplay between eccentricity and inclination due to angular momentum transfer. The period of the eccentricity and inclination oscillations for most observable configurations lie well within a main-sequence star lifetime, thus at least thousands of such oscillations may occur before the star evolves. The period is of the order of (*Kiseleva et al.* 1998):

$$\tau_{kozai} = \frac{2P_{out}^2}{3\pi P_{in}} \frac{M_1+M_2+M_3}{M_3}\left(1-e_{out}^2\right)^{3/2} \tag{10}$$

where M_1 and M_2 are the masses of the innermost two bodies orbiting each other with period $P_{\rm in}$ and M_3 is the mass of the outermost body orbiting the inner binary with period $P_{\rm out}$ and eccentricity $e_{\rm out}$.

Recent work has demonstrated that the approximations employed above fail to reproduce important aspects of the true motion, which can be modeled with 3-body numerical simulations. By instead retaining the octupole term in the disturbing function, *Ford et al.* (2000) derived more accurate, albeit complex, evolution equations for the true motion. Subsequent relaxation of the assumption of small initial eccentricities has allowed for a wider region of phase space of the true motion to be reproduced by the Lidov-Kozai mechanism (*Katz et al.* 2011; *Lithwick and Naoz* 2011; *Naoz et al.* 2011; *Libert and Delsate* 2012).

One outstanding consequence of retaining the octupole term is that the effect may flip a planet's orbital evolution from prograde to retrograde, and consequently may explain observations. The projected angle between stellar rotation and planetary orbital angular momentum has been measured for tens of hot Jupiters with the Rossiter-Mclaughlin effect (*Triaud et al.* 2010). These observations show us that some 20% of hot jupiters most probably have retrograde orbits whilst 50% or so are aligned (*Albrecht et al.* 2012). In at least one case (*Winn et al.* 2009) the true angle is at least $86°$, helping to reinforce indications of a subset of planets orbiting in a retrograde fashion with inclinations above $90°$ (*Albrecht et al.* 2012). *Naoz et al.* (2011) demonstrated how the Lidov-Kozai mechanism can produce these orbits[2]. Figure 6 illustrates how this inclination "flipping" can occur naturally in a three-body system, and the consequences of truncating the disturbing function to quadrupole order. In panel (a) and (b) of this figure, one sees that when the disturbing function is truncated at the quadrupole term, then the spread of inclinations and eccentricities are small, whereas when going to octupole order, the orbit flips (ie inclinations above $90°$) and eccentricities reach to values very close to unity.

[2]They also discovered an important error in the original derivation of the truncated, averaged disturbing function (*Kozai* 1962) which did not conserve angular momentum due to an erroneous assumption about the longitudes of ascending nodes.

Lidov-Kozai oscillations do not work in isolation. Bodies are not point masses: effects of tides, stellar oblateness and general relativity may play crucial roles in the evolution. These contributions have been detailed by *Fabrycky and Tremaine* (2007), *Chang* (2009), *Veras and Ford* (2010) and *Beust et al.* (2012).

A major consequence of these effects, in particular tides, is that planets formed beyond the snow line may become hot Jupiters through orbital shrinkage and tidal circularization [see Section 8].

The Lidov-Kozai mechanism may also be affected by the presence of a nascent protoplanetary disc, and hence play a crucial role during the formation of planets around one component of a binary system. If the secondary star is sufficiently inclined to and separated from the orbital plane of the primary, then the Lidov-Kozai mechanism might "turn on", exciting the eccentricity of planetesimals and diminishing prospects for planet formation (*Marzari and Barbieri* 2007; *Fragner et al.* 2011). However, the inclusion of the effects of gas drag (*Xie et al.* 2011) and protoplanetary disc self-gravity (*Batygin et al.* 2011) assuage the destructive effect of Lidov-Kozai oscillations, helping to provide favorable conditions for planetary growth.

Lidov-Kozai-like oscillations are also active in systems with more than three bodies, which is the focus of the remainder of this section. Examples include quadruple star systems (*Beust and Dutrey* 2006), triple star systems with one planet (*Marzari and Barbieri* 2007) and multiple-planet systems with or without additional stellar companions.

Given the likelihood of multiple exoplanets in binary systems, how the Lidov-Kozai mechanism operates in these systems is of particular interest. In particular, eccentricity and inclination oscillations produced by a wide-binary stellar companion can induce planet-planet scattering, leading to dynamical instability (*Innanen et al.* 1997). *Malmberg et al.* (2007a) demonstrate that this type of instability can result in planet stripping in the stellar birth cluster, where binaries are formed and disrupted at high inclinations.

Alternatively, multiple-planet systems within a wide binary may remain stable due to Lidov-Kozai oscillations. Understanding the conditions in which stability may occur and the consequences for the orbital system evolution can help explain current observations. *Takeda et al.* (2008) outline how to achieve this characterization by considering the secular evolution of a two-planet system in a wide binary, such that the mutual planet-planet interactions produce no change in semimajor axis. These planet-planet interactions may be coupled analytically to Lidov-Kozai oscillations because the latter are usually considered to result from secular evolution.

Takeda et al. (2008) compare the period of Lidov-Kozai oscillations with the period the oscillations produced by Laplace-Lagrange secular interactions (see Section 2), as shown in Figure 7. The figure provides an example of where Lidov-Kozai oscillations dominate or become suppressed (by comparing the curves), and the character of the resulting dynamical evolution (identified by the shaded regions). Because the Lidov-Kozai oscillation timescale increases with binary separation (see Equation 10), Lidov-Kozai oscillations are less likely to have an important effect on multi-planet evolution contained in wider stellar binaries. However, for wide-enough binaries, Galactic tides can cause close pericenter passages every few Gyr, perhaps explaining the difference in the observed eccentricity distribution of the population of giant planets in close binaries versus those in wide binaries (*Kaib et al.* 2013).

8. DYNAMICAL ORIGIN OF HOT JUPITERS

The first exoplanet that was confirmed to orbit a main sequence star, 51 Pegasi b (*Mayor and Queloz* 1995) became a prototype for a class of exoplanets known as hot Jupiters. The transiting subset of the hot Jupiters (here defined as $a \leq 0.1$ AU and $M_p \sin i = 0.25 - 20 M_J$) provide unique constraints on planetary evolution, and allow observational studies of atmospheric phenomena that are currently not possible for more distant planets. Identifying the dynamical origin of hot-Jupiters is a long-standing problem and is the topic of this section.

It is generally accepted that hot Jupiters cannot form *in situ* (*Bodenheimer et al.* 2000). If true, then their origin requires either migration through a massive, and presumably gaseous, disk or dynamical interactions involving multiple stellar or planetary bodies. Although both possibilities remain open, recent observations (e.g., *Winn et al.* 2010) indicate that roughly one fourth of hot Jupiter orbits are substantially misaligned with respect to the stellar rotation axis. These systems (and perhaps others) are naturally explained by dynamical processes, which are the focus of this section. The relevant dynamics may involve:

- Lidov-Kozai evolution of a one-planet system perturbed by a binary stellar companion
- Lidov-Kozai evolution in a multiple-planet system
- Scattering of multiple planets or secular evolution unrelated to the Kozai resonance
- Secular chaos

All of these processes are likely to occur at some level, so the main open question is their relative contribution to forming the observed hot Jupiter population. In every case, tidal interactions — which are inevitable for planets with the orbital period of hot Jupiters — are required in order to shrink and circularize the orbit (*Ivanov and Papaloizou* 2004; *Guillochon et al.* 2011). Tides raised on the star are expected to dominate orbital decay, while tides raised on the planet are likely to dominate circularization. However, tides on both bodies can contribute significantly. Quantitative comparisons between theoretical models and observations are limited by considerable uncertainties in tidal

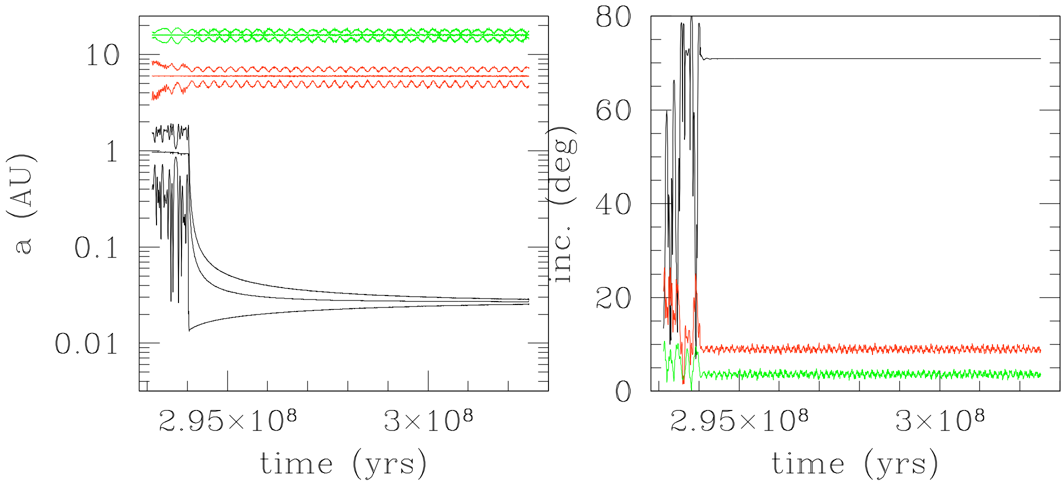

Fig. 10.— Hot Jupiter production by multiple planet evolution with no Lidov-Kozai cycles. The inner, middle and outer planets have masses of $0.5M_J$, $1.0M_J$ and $1.5M_J$, and initial semimajor axes of 1 AU, 6 AU and 16 AU, eccentricities of 0.066, 0.188 and 0.334 and inclinations of $4.5°$, $19.9°$ and $7.9°$. This choice places the AMD primarily in the outer planets (Figure 2 of *Wu and Lithwick* 2011, reproduced by permission of AAS).

physics and planetary structure, as well as observational biases in determining the orbital period distribution and the eccentricity of nearly circular orbits (*Zakamska et al.* 2011; *Gaidos and Mann* 2013).

A mechanism for generating high eccentricities, and tidal damping, are minimal ingredients for the dynamical formation of hot Jupiters. Several other processes, however, including general relativity, oblateness (*Correia et al.* 2012) and tides, can lead to precession of short-period orbits. These processes need to be included in models of hot Jupiter formation via secular dynamical effects. *Wu and Murray* (2003) quote formulae for the precession rates,

$$\begin{aligned}
\dot{\omega}_{GR} &= 3n\frac{GM_*}{a_p c^2(1-e_p^2)} \\
\dot{\omega}_{tid} &= \frac{15}{2}nk_2\frac{1+(3/2)e_p^2+(1/8)e_p^4}{(1-e_p^2)^5}\frac{M_*}{M_p}\left(\frac{R_p}{a_p}\right)^5 \\
\dot{\omega}_{obl} &= \frac{1}{2}n\frac{k_2}{(1-e_p^2)^2}\left(\frac{\Omega_p}{n}\right)^2\frac{M_*}{M_p}\left(\frac{R_p}{a_p}\right)^5. \qquad (11)
\end{aligned}$$

Here a_p, e_p, M_p, R_p and Ω_p are the planet's semi-major axis, eccentricity, mass, radius and spin frequency, n is the mean motion, and k_2 is the tidal Love number. Lidov-Kozai oscillations are generally suppressed if any of these precession rates exceed $\dot{\omega}_{kozai}$. This can easily occur for $a_p <$ 1 AU. Eccentricity can be enhanced when $\dot{\omega}_{GR} \simeq -\dot{\omega}_{kozai}$ (*Ford et al.* 2000).

Figure 8, from *Wu and Murray* (2003), illustrates how hot Jupiters can form in a single planet system with an inclined stellar companion. Lidov-Kozai oscillations in the planetary eccentricity result in periods where the pericenter distance is close enough for stellar tides to shrink the orbit. As the orbit shrinks, the additional dynamical effects described above become more important, resulting in a decrease in the amplitude of the eccentricity and inclination variations. In this example, after 700 Myr, GR suppresses the Lidov-Kozai oscillations completely. The influence of the secondary star then becomes negligible as tidal interactions dominate. *Wu et al.* (2007), using a binary population model and estimates for the radial distribution of massive extrasolar planets, estimated that this process could account for 10% or more of the hot Jupiter population.

A combination of gravitational scattering (*Ford and Rasio* 2006) and Lidov-Kozai oscillations can also lead to the production of hot Jupiters from multiple-planet systems around single stars. Figure 9 provides an example of three-planet scattering in which the outer planet is ejected, triggering Lidov-Kozai cycles between the other two planets. These oscillations are not as regular as those in Figure 6 because in Figure 9 the outermost body is comparable in mass to the middle body. Nevertheless, the oscillations of the argument of pericenter about $90°$ is indicative of the Lidov-Kozai mechanism at work. By about 3 Myr, the semimajor axis of the inner planet has shrunk to a value of 0.07 AU, after which other physical effects dictate the future evolution of the planet.

Both the fraction of scattering systems that yield star-grazing planets, and the fraction of those systems that yield surviving hot Jupiters, are uncertain. *Nagasawa et al.* (2008) and *Nagasawa and Ida* (2011) integrated ensembles of unstable three planet systems, using a model that included both gravitational and tidal forces. They obtained an extremely high yield ($\simeq$ 30%) of highly eccentric planets, that was larger than the yield found in earlier calculations that did not include tides (*Chatterjee et al.* 2008). One should note that these numbers do not reflect the expected fraction of scattering systems that would yield *long-lived* hot Jupiters, as many of the highly eccentric planets circularize into orbits with tidal decay times less than the main sequence lifetime. *Beaugé and Nesvorný* (2012), on

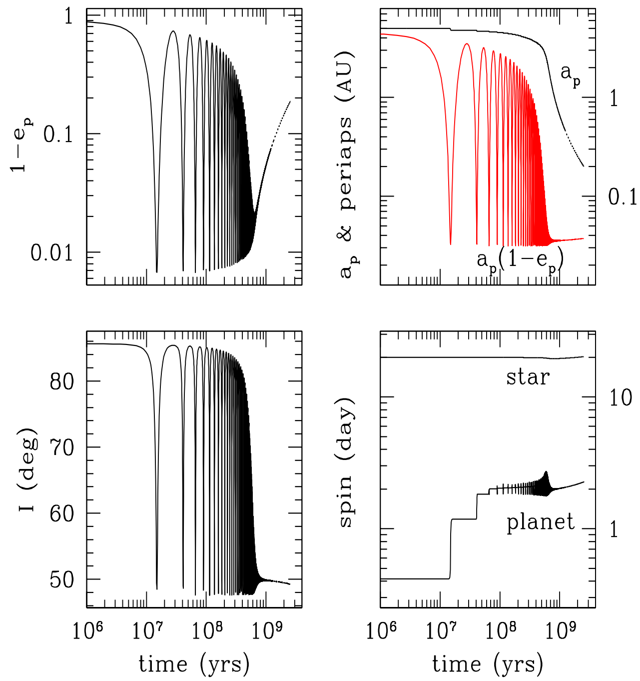

Fig. 8.— Hot Jupiter production by Lidov-Kozai forcing from a stellar binary companion. A $7.80 M_J$ planet with $a_p = 5.0$ AU, $e_p(t = 0) = 0.1$, $I_p(t = 0) = 85.6°$, and $\omega_p(t = 0) = 45°$ is evolving under the influence of two $1.1 M_\odot$ stars separated by 1000 AU on a $e_B = 0.5$ orbit (Figure1 of *Wu and Murray* 2003, reproduced by permission of AAS).

the other hand, using a different tidal model, a dispersion in planet masses, and resonant initial conditions, found a yield of surviving hot Jupiters of approximately 10%. Ten percent is also, roughly, the fraction of hot Jupiters in an unbiased sample of all massive planets with orbital radii less than a few AU. The efficiency of hot Jupiter production from scattering plus tidal circularization is thus high enough for this channel to contribute substantially to the population, if one assumes that scattering occurs in the majority of all such planetary systems.

Hot Jupiters can originate from multi-planet dynamics without the Lidov-Kozai effect. *Wu and Lithwick* (2011) present special configurations of the 4-body problem that allow for the innermost planet in a 3-planet system to be forced into the tidal circularization radius. These configurations require a significant angular momentum deficit (AMD) in the original planetary system. Figure 10 presents an example of hot Jupiter production without the Lidov-Kozai effect. Note that all three planets survive the evolution and never cross orbits.

If planet formation produces multiple planets on nearly circular, coplanar orbits, then secular evolution alone is not sufficient to produce hot Jupiters. Planet-disk interactions

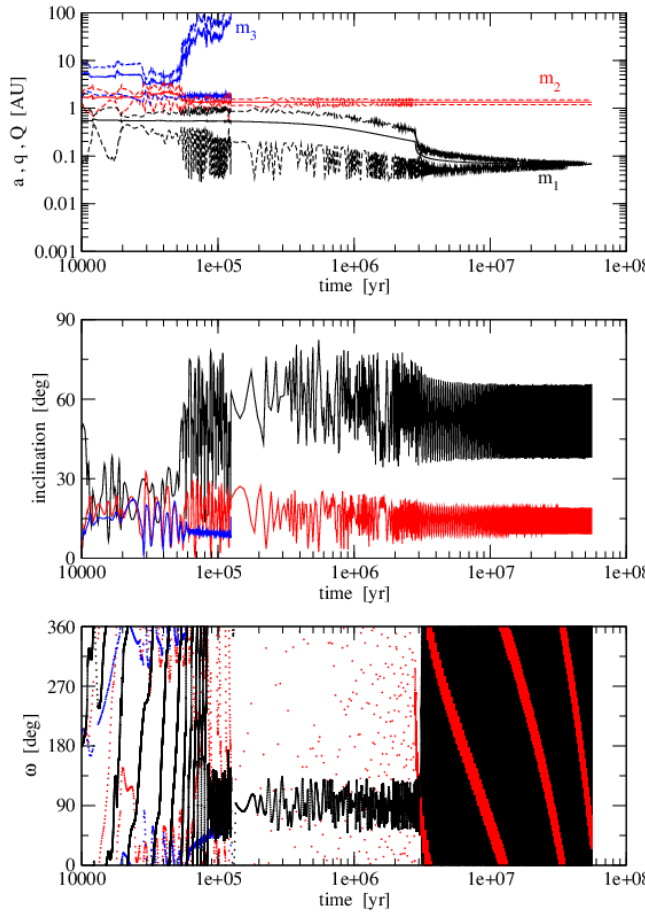

Fig. 9.— Hot Jupiter production by Lidov-Kozai forcing from multiple-planet interactions. The inner, middle and outer planets have masses of $1M_J$, $2M_J$ and $1M_J$ and initially nearly circular ($e < 0.1$) and coplanar ($I < 1°$) orbits (Figure 11 of *Beaugé and Nesvorný* 2012, reproduced by permission of AAS).

are not currently thought to be able to generate significant planetary eccentricity (except for high mass planets), and hence the easiest route toward forming systems with a significant AMD appears to be an initial phase of strong planet-planet scattering. In such a model, hot Jupiters could either be formed early (from highly eccentric scattered planets) or late (from long term secular evolution among the remaining planets after scattering). Which channel would dominate is unclear.

The observation of strongly misaligned and retrograde orbits from Rossiter-McLaughlin measurements provides evidence in favor of dynamical formation mechanisms (e.g., *Winn et al.* 2009), but does not immediately discriminate among different dynamical scenarios. In particular, although pure Lidov-Kozai evolution involving a circular stellar companion cannot create a retrograde planet, the presence of eccentricity in either a stellar or planetary perturber can (*Katz et al.* 2011; *Lithwick and Naoz* 2011). The same is true for secular evolution without the Lidov-Kozai effect.

Dawson et al. (2012b) compare the three potential origin channels described above, and suggest that Lidov-Kozai evolution in binary stellar systems is unlikely to dominate, but may explain $15^{+29}_{-11}\%$ of hot Jupiters, corroborating *Naoz et al.* (2012) result of $\approx 30\%$. These estimates rely upon the results of *Nagasawa and Ida* (2011) that find a large fraction of scattering systems ($\sim 30\%$) form (at least initially) a hot Jupiter, a result that they attribute in substantial part to Lidov-Kozai evolution. Similar calculations by *Beaugé and Nesvorný* (2012), using a more realistic tidal model, find less efficient hot Jupiter formation driven primarily by scattering events. They suggest that higher initial planetary multiplicity results in hot Jupiter populations in better accord with observations. *Morton and Johnson* (2011) provide constraints on the frequency of the two different Lidov-Kozai-induced hot Jupiter formation scenarios from spin-orbit data. They find that the results depend critically on the presence or lack of a population of aligned planetary systems. If this population exists, multiple-planet Lidov-Kozai scattering (specifically from the model of *Nagasawa et al.* 2008) is the favored formation mechanism. Otherwise, binary-induced Lidov-Kozai evolution (specifically from the model of *Fabrycky and Tremaine* 2007) is the favored model. The above results also depend upon the assumed tidal physics. *Dawson et al.* (2012a) identified Kepler Object of Interest (KOI) 1474.01 as a proto-hot Jupiter based on the long transit duration for its orbital period. The presence of large transit timing variations suggests that scattering by a more distant giant planet may explain the origin of KOI 1474.01's high eccentricity. With further analysis, the abundance of transiting proto-hot Jupiters could provide a constraint on the timescale of the high eccentricity migration phase of hot Jupiter's formation.

9. SUMMARY

We have reviewed the long-term dynamical evolution of planetary systems. Our key points are listed below:

1. *The giant-planet sub-system of the Solar System is stable* although the terrestrial-planet sub-system is marginally unstable with a small chance of planet-planet encounters during the lifetime of the Sun.

2. *Planet-planet scattering* in tighter planetary systems can lead to close encounters between planets. The timescale before a system undergoes such encounters is a strong function of the separation of planets.

3. *Secular interactions* cause the redistribution of angular momentum amongst planets in a system. In systems with a sufficiently large angular momentum deficit (AMD), such redistribution can lead to close planetary encounters.

4. *The outcome of planetary close encounters* is a function of the Safronov number. Collisions dominate when the planetary surface escape speeds are smaller than orbital speeds. Planetary scattering will be more common when the surface escape speeds are larger than the planetary orbital speeds in a system.

5. *Planets are predicted to pass through a phase of wide orbits* within unstable planetary systems as ejections occur only after several scatterings. Imaging surveys will therefore inform us about the frequency of unstable systems.

6. *The observed eccentricity distribution* is consistent with being an outcome of planet-planet scattering in unstable systems.

7. *Interactions with planetesimal disks* will cause planets to migrate which in turn can lead to instabilities within a planetary system. This process probably played an important role in the early history of our own Solar System.

8. *Aging systems may become unstable* when the host star evolves to become a white dwarf, and loses mass, as the relative strength of the planet-planet interactions increase compared to the interactions between the planets and host star.

9. *Fly-by encounters in stellar clusters* will occur in dense birth environments. Such encounters may lead to the direct ejection of planets in some cases. In other encounters, perturbations to the planetary orbits lead to instabilities on longer timescales. The intruding star may also pick-up a planet from the system.

10. *Exchange into binaries* can occur in stellar clusters. Planetary systems may be de-stabilised by the perturbing effect of the companion star through the Lidov-Kozai mechanism where the outer planet suffers periods of higher eccentricity leading it to have strong encounters with other planets.

11. *The Lidov-Kozai mechanism* may also operate within primordial binaries or planetary multiple systems, leading to the periodic increase in eccentricity of planet's orbits and planet-planet encounters in the case of multiple-planet systems.

12. *The origin of hot Jupiters* through dynamical interactions may involve one of five possible routes: Lidov-Kozai evolution of a one-planet system perturbed by a binary stellar companion; Lidov-Kozai evolution in a multiple-planet system; scattering of multiple planets; secular evolution unrelated to the Kozai resonance; or the re-orientation of circumstellar disks before planets form via interaction with a companion star, or via late infall of material or interactions or neighboring stars in clustered birth environments.

Acknowledgments. MBD was supported by the Swedish Research Council (grants 2008-4089 and 2011-3991). PJA acknowledges support from NASA grants NNX11AE12G and NNX13AI58G, and from grant HST-AR-12814 awarded by the Space Telescope Science Institute, which is operated by the Association of Universities for Research in Astronomy, Inc., for NASA, under contact NAS 5-26555. JC would like to thank NASA's Origins of Solar Systems program for support. EBF was supported by the National Aeronautics and Space Administration under Origins of Solar Systems grant NNX09AB35G and grants NNX08AR04G and NNX12AF73G issued through the Kepler Participating Scientist Program. We thank the anonymous referee for their useful comments.

REFERENCES

Adams F. C. (2010) *Annu. Rev. Astron. Astrophys.*, *48*, 47.

Adams F. C. and Laughlin G. (2001) *Icarus*, *150*, 151.

Adams F. C. and Laughlin G. (2003) *Icarus*, *163*, 290.

Adams F. C., Proszkow E. M., Fatuzzo M., and Myers P. C. (2006) *Astrophys. J.*, *641*, 504.

Adams F. C. and Shu F. H. (1986) *Astrophys. J.*, *308*, 836.

Albrecht S., Winn J. N., Johnson J. A., Howard A. W., Marcy G. W., Butler R. P. et al. (2012) *Astrophys. J.*, *757*, 18.

Allison R. J., Goodwin S. P., Parker R. J., de Grijs R., Portegies Zwart S. F., and Kouwenhoven M. B. N. (2009) *Astrophys. J. Lett.*, *700*, L99.

Barnes R. and Greenberg R. (2006a) *Astrophys. J. Lett.*, *652*, L53.

Barnes R. and Greenberg R. (2006b) *Astrophys. J. Lett.*, *647*, L163.

Bate M. R., Lodato G., and Pringle J. E. (2010) *Mon. Not. R. Astron. Soc.*, *401*, 1505.

Batygin K. (2012) *Nature*, *491*, 418.

Batygin K. and Brown M. E. (2010) *Astrophys. J.*, *716*, 1323.

Batygin K., Brown M. E., and Betts H. (2012) *Astrophys. J. Lett.*, *744*, L3.

Batygin K. and Laughlin G. (2008) *Astrophys. J.*, *683*, 1207.

Batygin K., Morbidelli A., and Tsiganis K. (2011) *Astron. Astrophys.*, *533*, A7.

Beaugé C. and Nesvorný D. (2012) *Astrophys. J.*, *751*, 119.

Beust H., Bonfils X., Montagnier G., Delfosse X., and Forveille T. (2012) *Astron. Astrophys.*, *545*, A88.

Beust H. and Dutrey A. (2006) *Astron. Astrophys.*, *446*, 137.

Binney J. and Tremaine S. (1987) *Galactic dynamics*.

Blaes O., Lee M. H., and Socrates A. (2002) *Astrophys. J.*, *578*, 775.

Bodenheimer P., Hubickyj O., and Lissauer J. J. (2000) *Icarus*, *143*, 2.

Boley A. C., Payne M. J., and Ford E. B. (2012) *Astrophys. J.*.

Bonnell I. A., Smith K. W., Davies M. B., and Horne K. (2001) *Mon. Not. R. Astron. Soc.*, *322*, 859.

Booth M., Wyatt M. C., Morbidelli A., Moro-Martín A., and Levison H. F. (2009) *Mon. Not. R. Astron. Soc.*, *399*, 385.

Bottke W. F., Vokrouhlický D., Minton D., Nesvorný D., Morbidelli A., Brasser R. et al. (2012) *Nature*, *485*, 78.

Brasser R., Duncan M. J., and Levison H. F. (2007) *Icarus*, *191*, 413.

Brasser R. and Morbidelli A. (2013) *ArXiv e-prints*.

Butler R. P., Wright J. T., Marcy G. W., Fischer D. A., Vogt S. S., Tinney C. G. et al. (2006) *Astrophys. J.*, *646*, 505.

Capobianco C. C., Duncan M., and Levison H. F. (2011) *Icarus*, *211*, 819.

Cassen P. and Moosman A. (1981) *Icarus*, *48*, 353.

Chambers J. E., Wetherill G. W., and Boss A. P. (1996) *Icarus*, *119*, 261.

Chandar R., Bianchi L., and Ford H. C. (1999) *Astrophys. J. Suppl.*, *122*, 431.

Chang P. (2009) *Mon. Not. R. Astron. Soc.*, *393*, 224.

Chatterjee S., Ford E. B., Matsumura S., and Rasio F. A. (2008) *Astrophys. J.*, *686*, 580.

Chiang E. and Laughlin G. (2013) *Mon. Not. R. Astron. Soc.*, *431*, 3444.

Ciardi D. R., Fabrycky D. C., Ford E. B., Gautier III T. N., Howell S. B., Lissauer J. J. et al. (2013) *Astrophys. J.*, *763*, 41.

Correia A. C. M., Boué G., and Laskar J. (2012) *Astrophys. J. Lett.*, *744*, L23.

Cresswell P., Dirksen G., Kley W., and Nelson R. P. (2007) *Astron. Astrophys.*, *473*, 329.

D'Angelo G., Lubow S. H., and Bate M. R. (2006) *Astrophys. J.*, *652*, 1698.

Davies M. B. and Sigurdsson S. (2001) *Mon. Not. R. Astron. Soc.*, *324*, 612.

Dawson R. I., Johnson J. A., Morton T. D., Crepp J. R., Fabrycky D. C., Murray-Clay R. A. et al. (2012a) *Astrophys. J.*, *761*, 163.

Dawson R. I., Murray-Clay R. A., and Johnson J. A. (2012b) *ArXiv e-prints*.

Debes J. H. and Sigurdsson S. (2002) *Astrophys. J.*, *572*, 556.

Debes J. H., Walsh K. J., and Stark C. (2012) *Astrophys. J.*, *747*, 148.

Duncan M. J. and Lissauer J. J. (1998) *Icarus*, *134*, 303.

Dunhill A. C., Alexander R. D., and Armitage P. J. (2013) *Mon. Not. R. Astron. Soc.*, *428*, 3072.

Fabrycky D. and Tremaine S. (2007) *Astrophys. J.*, *669*, 1298.

Fang J. and Margot J.-L. (2012a) *Astrophys. J.*, *761*, 92.

Fang J. and Margot J.-L. (2012b) *Astron. J.*, *143*, 59.

Fernandez J. A. and Ip W.-H. (1984) *Icarus*, *58*, 109.

Ford E. B. (2005) *Astron. J.*, *129*, 1706.

Ford E. B., Havlickova M., and Rasio F. A. (2001) *Icarus*, *150*, 303.

Ford E. B., Kozinsky B., and Rasio F. A. (2000) *Astrophys. J.*, *535*, 385.

Ford E. B., Lystad V., and Rasio F. A. (2005) *Nature*, *434*, 873.

Ford E. B. and Rasio F. A. (2006) *Astrophys. J. Lett.*, *638*, L45.

Ford E. B. and Rasio F. A. (2008) *Astrophys. J.*, *686*, 621.

Ford E. B., Rasio F. A., and Yu K. (2003) in: *Scientific Frontiers in Research on Extrasolar Planets*, vol. 294 of *Astronomical Society of the Pacific Conference Series*, (edited by D. Deming and S. Seager), pp. 181–188.

Fragner M. M., Nelson R. P., and Kley W. (2011) *Astron. Astrophys.*, *528*, A40.

Gaidos E. and Mann A. W. (2013) *Astrophys. J.*, *762*, 41.

Gallardo T. (2006) *Icarus*, *181*, 205.

Gallardo T., Hugo G., and Pais P. (2012) *Icarus*, *220*, 392.

Gladman B. (1993) *Icarus*, *106*, 247.

Goldreich P., Lithwick Y., and Sari R. (2004) *Astrophys. J.*, *614*, 497.

Gomes R., Levison H. F., Tsiganis K., and Morbidelli A. (2005) *Nature*, *435*, 466.

Gomes R. S., Morbidelli A., and Levison H. F. (2004) *Icarus*, *170*, 492.

Gopakumar A., Bagchi M., and Ray A. (2009) *Mon. Not. R. Astron. Soc.*, *399*, L123.

Gounelle M., Chaussidon M., and Rollion-Bard C. (2013) *Astrophys. J. Lett.*, *763*, L33.

Gounelle M. and Meynet G. (2012) *Astron. Astrophys.*, *545*, A4.
Guillochon J., Ramirez-Ruiz E., and Lin D. (2011) *Astrophys. J.*, *732*, 74.
Guzzo M. (2005) *Icarus*, *174*, 273.
Hahn J. M. and Malhotra R. (1999) *Astron. J.*, *117*, 3041.
Hao W., Kouwenhoven M. B. N., and Spurzem R. (2013) *Mon. Not. R. Astron. Soc.*.
Hartmann W. K., Ryder G., Dones L., and Grinspoon D. (2000) *The Time-Dependent Intense Bombardment of the Primordial Earth/Moon System*, pp. 493–512.
Hayes W. B. (2008) *Mon. Not. R. Astron. Soc.*, *386*, 295.
Heller C. H. (1995) *Astrophys. J.*, *455*, 252.
Hester J. J., Desch S. J., Healy K. R., and Leshin L. A. (2004) *Science*, *304*, 1116.
Innanen K. A., Zheng J. Q., Mikkola S., and Valtonen M. J. (1997) *Astron. J.*, *113*, 1915.
Ivanov P. B. and Papaloizou J. C. B. (2004) *Mon. Not. R. Astron. Soc.*, *347*, 437.
Johansen A., Davies M. B., Church R. P., and Holmelin V. (2012) *Astrophys. J.*, *758*, 39.
Jones H. R. A., Butler R. P., Tinney C. G., Marcy G. W., Carter B. D., Penny A. J. et al. (2006) *Mon. Not. R. Astron. Soc.*, *369*, 249.
Jurić M. and Tremaine S. (2008) *Astrophys. J.*, *686*, 603.
Kaib N. A. and Quinn T. (2009) *Science*, *325*, 1234.
Kaib N. A., Raymond S. N., and Duncan M. (2013) *Nature*, *493*, 381.
Katz B., Dong S., and Malhotra R. (2011) *Physical Review Letters*, *107*, 18, 181101.
Kenyon S. J. and Bromley B. C. (2004) *Nature*, *432*, 598.
Kirsh D. R., Duncan M., Brasser R., and Levison H. F. (2009) *Icarus*, *199*, 197.
Kiseleva L. G., Eggleton P. P., and Mikkola S. (1998) *Mon. Not. R. Astron. Soc.*, *300*, 292.
Kley W. and Dirksen G. (2006) *Astron. Astrophys.*, *447*, 369.
Kley W., Lee M. H., Murray N., and Peale S. J. (2005) *Astron. Astrophys.*, *437*, 727.
Kley W. and Nelson R. P. (2012) *Annu. Rev. Astron. Astrophys.*, *50*, 211.
Kobayashi H. and Ida S. (2001) *Icarus*, *153*, 416.
Kokubo E. and Ida S. (1998) *Icarus*, *131*, 171.
Kozai Y. (1962) *Astron. J.*, *67*, 591.
Kozai Y. (1985) *Celestial Mechanics*, *36*, 47.
Kring D. A. and Cohen B. A. (2002) *Journal of Geophysical Research (Planets)*, *107*, 5009.
Kuchner M. J. (2004) *Astrophys. J.*, *612*, 1147.
Lada C. J. and Lada E. A. (2003) *Annu. Rev. Astron. Astrophys.*, *41*, 57.
Lagrange A.-M., Backman D. E., and Artymowicz P. (2000) *Protostars and Planets IV*, p. 639.
Laskar J. (1989) *Nature*, *338*, 237.
Laskar J. (1990) *Icarus*, *88*, 266.
Laskar J. (1994) *Astron. Astrophys.*, *287*, L9.
Laskar J. (1997) *Astron. Astrophys.*, *317*, L75.
Laskar J. (2008) *Icarus*, *196*, 1.
Laskar J. and Gastineau M. (2009) *Nature*, *459*, 817.
Laughlin G. and Adams F. C. (1998) *Astrophys. J. Lett.*, *508*, L171.
Laughlin G. and Adams F. C. (2000) *Icarus*, *145*, 614.
Lee M. H. and Peale S. J. (2002) *Astrophys. J.*, *567*, 596.
Lega E., Morbidelli A., and Nesvorný D. (2013) *Mon. Not. R. Astron. Soc.*, *431*, 3494.
Levison H. F., Morbidelli A., Gomes R., and Backman D. (2007) *Protostars and Planets V*, pp. 669–684.
Levison H. F., Morbidelli A., Tsiganis K., Nesvorný D., and Gomes R. (2011) *Astron. J.*, *142*, 152.
Levison H. F., Morbidelli A., Van Laerhoven C., Gomes R., and Tsiganis K. (2008) *Icarus*, *196*, 258.
Levison H. F., Thommes E., and Duncan M. J. (2010) *Astron. J.*, *139*, 1297.
Libert A.-S. and Delsate N. (2012) *Mon. Not. R. Astron. Soc.*, *422*, 2725.
Lidov M. L. (1962) *Planet. Space Sci.*, *9*, 719.
Lin D. N. C. and Ida S. (1997) *Astrophys. J.*, *477*, 781.
Lissauer J. J. (1995) *Icarus*, *114*, 217.
Lissauer J. J., Ragozzine D., Fabrycky D. C., Steffen J. H., Ford E. B., Jenkins J. M. et al. (2011) *Astrophys. J. Suppl.*, *197*, 8.
Lithwick Y. and Naoz S. (2011) *Astrophys. J.*, *742*, 94.
Malmberg D. and Davies M. B. (2009) *Mon. Not. R. Astron. Soc.*, *394*, L26.
Malmberg D., Davies M. B., and Chambers J. E. (2007a) *Mon. Not. R. Astron. Soc.*, *377*, L1.
Malmberg D., Davies M. B., and Heggie D. C. (2011) *Mon. Not. R. Astron. Soc.*, *411*, 859.
Malmberg D., de Angeli F., Davies M. B., Church R. P., Mackey D., and Wilkinson M. I. (2007b) *Mon. Not. R. Astron. Soc.*, *378*, 1207.
Marchal C. and Bozis G. (1982) *Celestial Mechanics*, *26*, 311.
Marchi S., Bottke W. F., Kring D. A., and Morbidelli A. (2012a) *Earth and Planetary Science Letters*, *325*, 27.
Marchi S., Bottke W. F., O'Brien D. P., Schenk P., Mottola S., De Sanctis M. C. et al. (2013) *ArXiv e-prints*.
Marchi S., McSween H. Y., O'Brien D. P., Schenk P., De Sanctis M. C., Gaskell R. et al. (2012b) *Science*, *336*, 690.
Marzari F. and Barbieri M. (2007) *Astron. Astrophys.*, *472*, 643.
Marzari F., Baruteau C., and Scholl H. (2010) *Astron. Astrophys.*, *514*, L4.
Marzari F. and Weidenschilling S. J. (2002) *Icarus*, *156*, 570.
Matsumoto Y., Nagasawa M., and Ida S. (2012) *Icarus*, *221*, 624.
Matsumura S., Ida S., and Nagasawa M. (2013) *Astrophys. J.*, *767*, 129.
Matsumura S., Thommes E. W., Chatterjee S., and Rasio F. A. (2010) *Astrophys. J.*, *714*, 194.
Mayor M. and Queloz D. (1995) *Nature*, *378*, 355.
Moeckel N. and Armitage P. J. (2012) *Mon. Not. R. Astron. Soc.*, *419*, 366.
Moeckel N., Raymond S. N., and Armitage P. J. (2008) *Astrophys. J.*, *688*, 1361.
Moorhead A. V. and Adams F. C. (2005) *Icarus*, *178*, 517.
Morbidelli A., Brasser R., Gomes R., Levison H. F., and Tsiganis K. (2010) *Astron. J.*, *140*, 1391.
Morbidelli A. and Froeschlé C. (1996) *Celestial Mechanics and Dynamical Astronomy*, *63*, 227.
Morbidelli A. and Levison H. F. (2004) *Astron. J.*, *128*, 2564.
Morbidelli A., Tsiganis K., Crida A., Levison H. F., and Gomes R. (2007) *Astron. J.*, *134*, 1790.
Morton T. D. and Johnson J. A. (2011) *Astrophys. J.*, *729*, 138.
Murray C. D. and Dermott S. F. (1999) *Solar system dynamics*.
Mustill A. J. and Wyatt M. C. (2012) *Mon. Not. R. Astron. Soc.*, *419*, 3074.
Nagasawa M. and Ida S. (2011) *Astrophys. J.*, *742*, 72.
Nagasawa M., Ida S., and Bessho T. (2008) *Astrophys. J.*, *678*, 498.
Naoz S., Farr W. M., Lithwick Y., Rasio F. A., and Teyssandier J.

(2011) *Nature*, *473*, 187.
Naoz S., Farr W. M., and Rasio F. A. (2012) *Astrophys. J. Lett.*, *754*, L36.
Nesvorný D. and Morbidelli A. (2012) *Astron. J.*, *144*, 117.
Ostriker E. C. (1994) *Astrophys. J.*, *424*, 292.
Papaloizou J. C. B., Nelson R. P., and Masset F. (2001) *Astron. Astrophys.*, *366*, 263.
Papaloizou J. C. B. and Terquem C. (2001) *Mon. Not. R. Astron. Soc.*, *325*, 221.
Parker R. J. and Quanz S. P. (2012) *Mon. Not. R. Astron. Soc.*, *419*, 2448.
Perets H. B. and Naoz S. (2009) *Astrophys. J. Lett.*, *699*, L17.
Proszkow E.-M. and Adams F. C. (2009) *Astrophys. J. Suppl.*, *185*, 486.
Quillen A. C. (2011) *Mon. Not. R. Astron. Soc.*, *418*, 1043.
Rasio F. A. and Ford E. B. (1996) *Science*, *274*, 954.
Raymond S. N. and Armitage P. J. (2013) *Mon. Not. R. Astron. Soc.*, *429*, L99.
Raymond S. N., Armitage P. J., and Gorelick N. (2009a) *Astrophys. J. Lett.*, *699*, L88.
Raymond S. N., Armitage P. J., and Gorelick N. (2010) *Astrophys. J.*, *711*, 772.
Raymond S. N., Armitage P. J., Moro-Martín A., Booth M., Wyatt M. C., Armstrong J. C. et al. (2011) *Astron. Astrophys.*, *530*, A62.
Raymond S. N., Armitage P. J., Moro-Martín A., Booth M., Wyatt M. C., Armstrong J. C. et al. (2012) *Astron. Astrophys.*, *541*, A11.
Raymond S. N., Barnes R., Armitage P. J., and Gorelick N. (2008) *Astrophys. J. Lett.*, *687*, L107.
Raymond S. N., Barnes R., Veras D., Armitage P. J., Gorelick N., and Greenberg R. (2009b) *Astrophys. J. Lett.*, *696*, L98.
Ribas I. and Miralda-Escudé J. (2007) *Astron. Astrophys.*, *464*, 779.
Ryder G. (2002) *Journal of Geophysical Research (Planets)*, *107*, 5022.
Scharf C. and Menou K. (2009) *Astrophys. J. Lett.*, *693*, L113.
Schneider J., Dedieu C., Le Sidaner P., Savalle R., and Zolotukhin I. (2011) *Astron. Astrophys.*, *532*, A79.
Shappee B. J. and Thompson T. A. (2013) *Astrophys. J.*, *766*, 64.
Shen Y. and Turner E. L. (2008) *Astrophys. J.*, *685*, 553.
Smith A. W. and Lissauer J. J. (2009) *Icarus*, *201*, 381.
Spiegel D. S. and Burrows A. (2012) *Astrophys. J.*, *745*, 174.
Spurzem R., Giersz M., Heggie D. C., and Lin D. N. C. (2009) *Astrophys. J.*, *697*, 458.
Sumi T., Kamiya K., Bennett D. P., Bond I. A., Abe F., Botzler C. S. et al. (2011) *Nature*, *473*, 349.
Sussman G. J. and Wisdom J. (1988) *Science*, *241*, 433.
Sussman G. J. and Wisdom J. (1992) *Science*, *257*, 56.
Takeda G., Kita R., and Rasio F. A. (2008) *Astrophys. J.*, *683*, 1063.
Tera F., Papanastassiou D. A., and Wasserburg G. J. (1974) *Earth and Planetary Science Letters*, *22*, 1.
Thompson T. A. (2011) *Astrophys. J.*, *741*, 82.
Throop H. B. and Bally J. (2008) *Astron. J.*, *135*, 2380.
Timpe M. L., Barnes R., Raymond S. N., and Gorelick N. (2012) in: *American Astronomical Society Meeting Abstracts #219*, vol. 219 of *American Astronomical Society Meeting Abstracts*, p. #339.12.
Tremaine S. and Dong S. (2012) *Astron. J.*, *143*, 94.
Triaud A. H. M. J., Collier Cameron A., Queloz D., Anderson D. R., Gillon M., Hebb L. et al. (2010) *Astron. Astrophys.*, *524*, A25.
Tsiganis K., Gomes R., Morbidelli A., and Levison H. F. (2005) *Nature*, *435*, 459.
Udry S. and Santos N. C. (2007) *Annu. Rev. Astron. Astrophys.*, *45*, 397.
Valtonen M. and Karttunen H. (2006) *The Three-Body Problem*.
Vashkov'yak M. A. (1999) *Astronomy Letters*, *25*, 476.
Veras D. and Armitage P. J. (2005) *Astrophys. J. Lett.*, *620*, L111.
Veras D. and Armitage P. J. (2006) *Astrophys. J.*, *645*, 1509.
Veras D., Crepp J. R., and Ford E. B. (2009) *Astrophys. J.*, *696*, 1600.
Veras D. and Ford E. B. (2009) *Astrophys. J. Lett.*, *690*, L1.
Veras D. and Ford E. B. (2010) *Astrophys. J.*, *715*, 803.
Veras D. and Mustill A. J. (2013) *ArXiv e-prints*.
Veras D., Mustill A. J., Bonsor A., and Wyatt M. C. (2013) *Mon. Not. R. Astron. Soc.*, *431*, 1686.
Veras D. and Raymond S. N. (2012) *Mon. Not. R. Astron. Soc.*, *421*, L117.
Veras D., Wyatt M. C., Mustill A. J., Bonsor A., and Eldridge J. J. (2011) *Mon. Not. R. Astron. Soc.*, *417*, 2104.
Voyatzis G., Hadjidemetriou J. D., Veras D., and Varvoglis H. (2013) *Mon. Not. R. Astron. Soc.*, *430*, 3383.
Wadhwa M., Amelin Y., Davis A. M., Lugmair G. W., Meyer B., Gounelle M. et al. (2007) *Protostars and Planets V*, pp. 835–848.
Wan X.-S. and Huang T.-Y. (2007) *Mon. Not. R. Astron. Soc.*, *377*, 133.
Wasserburg G. J., Busso M., Gallino R., and Nollett K. M. (2006) *Nuclear Physics A*, *777*, 5.
Weidenschilling S. J. (1977) *Astrophys. Space Sci.*, *51*, 153.
Weidenschilling S. J. and Marzari F. (1996) *Nature*, *384*, 619.
Wiegert P. and Tremaine S. (1999) *Icarus*, *137*, 84.
Williams J. P. and Cieza L. A. (2011) *Annu. Rev. Astron. Astrophys.*, *49*, 67.
Winn J. N., Fabrycky D., Albrecht S., and Johnson J. A. (2010) *Astrophys. J. Lett.*, *718*, L145.
Winn J. N., Johnson J. A., Albrecht S., Howard A. W., Marcy G. W., Crossfield I. J. et al. (2009) *Astrophys. J. Lett.*, *703*, L99.
Wisdom J. (1980) *Astron. J.*, *85*, 1122.
Wright J. T., Fakhouri O., Marcy G. W., Han E., Feng Y., Johnson J. A. et al. (2011) *PASP*, *123*, 412.
Wright J. T., Upadhyay S., Marcy G. W., Fischer D. A., Ford E. B., and Johnson J. A. (2009) *Astrophys. J.*, *693*, 1084.
Wu Y. and Lithwick Y. (2011) *Astrophys. J.*, *735*, 109.
Wu Y. and Murray N. (2003) *Astrophys. J.*, *589*, 605.
Wu Y., Murray N. W., and Ramsahai J. M. (2007) *Astrophys. J.*, *670*, 820.
Wyatt M. C. (2008) *Annu. Rev. Astron. Astrophys.*, *46*, 339.
Xie J.-W., Payne M. J., Thébault P., Zhou J.-L., and Ge J. (2011) *Astrophys. J.*, *735*, 10.
Zakamska N. L., Pan M., and Ford E. B. (2011) *Mon. Not. R. Astron. Soc.*, *410*, 1895.
Zuckerman B. (2001) *Annu. Rev. Astron. Astrophys.*, *39*, 549.

This 2-column preprint was prepared with the AAS LaTeX macros v5.2.